# Supersaturation of Water Vapor in Clouds

ALEXEI V. KOROLEV

*Sky Tech Research, Inc., Richmond Hill, Ontario, Canada*

ILIA P. MAZIN

*Center for Earth and Space Research, George Mason University, Fairfax, Virginia*

(Manuscript received 18 October 2002, in final form 26 June 2003)

ABSTRACT

A theoretical framework is developed to estimate the supersaturation in liquid, ice, and mixed-phase clouds. An equation describing supersaturation in mixed-phase clouds in general form is considered here. The solution for this equation is obtained for the case of quasi-steady approximation, that is, when particle sizes stay constant. It is shown that the supersaturation asymptotically approaches the quasi-steady supersaturation over time. This creates a basis for the estimation of the supersaturation in clouds from the quasi-steady supersaturation calculations. The quasi-steady supersaturation is a function of the vertical velocity and size distributions of liquid and ice particles, which can be obtained from in situ measurements. It is shown that, in mixed-phase clouds, the evaporating droplets maintain the water vapor pressure close to saturation over water, which enables the analytical estimation of the time of glaciation of mixed-phase clouds. The limitations of the quasi-steady approximation in clouds with different phase composition are considered here. The role of phase relaxation time, as well as the effect of the characteristic time and spatial scales of turbulent fluctuations, are also discussed.

## 1. Introduction

The phase transition of water from vapor into liquid or solid phase plays a pivotal role in the formation of clouds and precipitation. The direction and rate of the phase transition ''liquid-to-vapor'' or ''ice-to-vapor'' are determined by the vapor supersaturation with respect to liquid or ice, respectively. The early numerical modeling by Howell (1949) and Mordy (1959) has shown that the supersaturation in a uniformly ascending cloud parcel reaches a maximum near the cloud base during activation of droplets and then monotonically decreases. Squires (1952) derived a relationship between supply and depletion of water vapor in a vertically moving cloud parcel. The solution of the Squires equation suggested that, to a first approximation, the supersaturation is linearly related to a vertical velocity and inversely proportional to the concentration and the average size of the cloud droplets. This relationship was later used to determine supersaturation in convective clouds by Warner (1968), Paluch and Knight (1984), and Politovich and Cooper (1988). The characteristic time of phase transition due to water vapor depletion by cloud droplets is inversely proportional to the product of droplet concentration and its average size (Squires 1952; Mazin 1966, 1968). Questions relating to the formation of supersaturation in clouds were discussed in great details by Kabanov et al. (1971). Rogers (1975) studied the supersaturation equation for liquid clouds numerically and considered analytical solutions for some special cases. Subsequent refinements of the supersaturation equation and the time of phase relaxation were made by Korolev (1994). Most studies of the supersaturation are related to liquid clouds. Only few works consider supersaturation in glaciated clouds (e.g., Juisto 1971; Heymsfield 1975).

The present paper is focused on a study of the supersaturation in clouds of any phase composition: mixed, liquid, and ice. In the section 2 we consider the equation for supersaturation in a general form for a three-phase component system consisting of water vapor, liquid, and ice particles. Section 3 presents a solution of the supersaturation equation for the case of quasi-steady approximation, that is, when the sizes of cloud particles stay constant. Sections 4 and 5 examine supersaturation in liquid, ice, and mixed-phase clouds. In section 6 the analytical solution for the glaciating time of mixed-phase clouds for zero vertical velocity is obtained. Section 7 justifies the possibility of estimating the in-cloud supersaturation from the quasi-steady supersaturation, which can be calculated from in situ measurements of particle size distributions and vertical velocity. In section 8 the limiting conditions for the results are discussed.

*Corresponding author address:* Alexei V. Korolev, Sky Tech Research, Inc., 28 Don Head Village Blvd., Richmond Hill, ON L4C 7M6, Canada.
E-mail: Alexei.Korolev@rogers.com

© 2003 American Meteorological Society

## 2. General equation

Consider a vertically moving adiabatic cloud parcel consisting of a mixture of liquid droplets and ice particles uniformly distributed in space. Assume that the cloud particles move with the air and stay inside the parcel at all times and no activation of new cloud droplets and nucleation of ice particles occur. Thus, the number of droplets and ice particles per unit mass of the air stays constant. Another assumption is related to so called *regular* condensation; that is, the water vapor pressure and temperature fields at large distance from cloud particles are considered to be uniform, and all cloud particles grow or evaporate under the same conditions.

The changes in the supersaturation in the cloud parcel can be described by an equation (appendix A):

$$\frac{1}{S_w + 1}\frac{dS_w}{dt} = \left(\frac{gL_w}{c_pR_vT^2} - \frac{g}{R_aT}\right)u_z - \left(\frac{1}{q_v} + \frac{L_w^2}{c_pR_vT^2}\right)\frac{dq_w}{dt} - \left(\frac{1}{q_v} + \frac{L_iL_w}{c_pR_vT^2}\right)\frac{dq_i}{dt}. \quad (1)$$

Here, $S_w = (e - E_w)/E_w$ is the supersaturation with respect to water; $e$ is the water vapor pressure; $E_w(T)$ is the saturated vapor pressure over liquid water at temperature $T$; $q_v$, $q_w$, and $q_i$ are the mixing ratios of water vapor, liquid water, and ice, respectively (mass per 1 kg of dry air); $R_v$ and $R_a$ are the specific gas constants of water vapor and air, respectively; $c_p$ is the specific heat capacitance of the air at constant pressure; $L_w$ and $L_i$ are the latent heat of water evaporation and ice sublimation, respectively; $g$ is the acceleration of gravity; $u_z$ is the vertical velocity of the cloud parcel.

The rate of changes in the liquid water mixing ratio due to condensation or evaporation of cloud droplets can be described as

$$\frac{dq_w}{dt} = \frac{4\pi\rho_wN_w}{\rho_a}\int_0^\infty f_w(r_w)r_w^2\frac{dr_w}{dt}\,dr_w. \quad (2)$$

Here, $f_w(r_w)$ is the size distribution of cloud droplets normalized to unity, $r_w$ is the droplet radius, $N_w$ is the number concentration of the cloud droplets, $\rho_w$ and $\rho_a$ are the densities of liquid water and dry air, respectively.

The mass transfer of water from vapor to liquid phase inside clouds is mainly related to droplets having $r_w > 1\ \mu$m. For such droplets, the corrections for the droplet curvature and salinity can be disregarded, and the equation for a droplet growth can be written as (e.g., Pruppacher and Klett 1997)

$$\frac{dr_w}{dt} = \frac{A_wS_w}{r_w}. \quad (3)$$

Here, $A_w = (\rho_wL_w^2/kR_vT^2 + \rho_wR_vT/E_wD)^{-1}$, $D$ is the coefficient of water vapor diffusion in the air, and $k$ is the coefficient of air heat conductivity. Substituting Eq. (3) into Eq. (2) and averaging over $r$ results in

$$\frac{dq_w}{dt} = B_wS_wN_w\bar{r}_w, \quad (4)$$

where $B_w = 4\pi\rho_wA_w/\rho_a$ and $\bar{r}_w$ is the average radius of cloud droplets.

Similarly, an equation for changes in the mixing ratio of ice can be written as

$$\frac{dq_i}{dt} = \frac{4\pi N_i}{\rho_a}\int_0^1\int_{\rho_{i\min}}^{\rho_{i\max}}\int_0^\infty f_i(r_i,\ \rho_i,\ c)\rho_ir^2\frac{dr_i}{dt}\,dr_i\,d\rho_i\,dc. \quad (5)$$

Here, $N_i$ is the number concentration of ice particles; $r_i$ is the characteristic size of ice particles; $c$ is a shape factor of ice particles characterizing ''capacitance'' in the equation of the growth rate; $\rho_i$ is the density of ice particles ($\rho_{i\min} < \rho_i < \rho_{i\max}$); and $f_i(r_i,\ \rho_i,\ c)$ is the distribution of ice particles by characteristic size, density, and shape factor normalized to unity. The size of an ice particle is an ambiguous parameter, and it can be defined in a number of different ways. The ice particle size $r_i$ is related to the shape factor $c$ through the rate of the mass growth. In the following consideration, the size $r_i$ will be defined as half the maximum dimension of the ice particle. For this definition of $r_i$, the shape factor varies in the range $0 < c \leq 1$, being equal to 1 for ice spheres.

Using Jeffery's electrostatic analogy, the diffusional growth rate of the ice particles can be written as (e.g., Pruppacher and Klett 1997)

$$\frac{dr_i}{dt} = \frac{cA_iS_i}{r_i}. \quad (6)$$

Here, $A_i = (\rho_iL_i^2/kR_vT^2 + \rho_iR_vT/E_iD)^{-1}$; $E_i$ is the saturated water vapor pressure over a flat ice surface at temperature $T$; $S_i$ is the supersaturation over ice.

The supersaturation over ice can be related to the supersaturation over water with

$$S_i = \frac{e - E_i}{E_i} = \xi S_w + \xi - 1, \quad (7)$$

where $\xi(T) = E_w(T)/E_i(T)$. Then, substituting Eqs. (6) and (7) into Eq. (5) and averaging over $r_i$ and $c$ gives

$$\frac{dq_i}{dt} = (\xi S_w + \xi - 1)\frac{4\pi A_iN_i\overline{r_ic}}{\rho_a},$$

which for simplicity yields

$$\frac{dq_i}{dt} = (B_iS_w + B_i^*)N_i\bar{r}_i \quad (8)$$

if one assumes that $c$ is the same for all ice particles and that

$$B_i = \frac{4\pi\rho_ic\xi A_i}{\rho_a}; \qquad B_i^* = \frac{4\pi\rho_ic}{\rho_a}(\xi - 1)A_i.$$

Substituting Eqs. (4) and (8) in Eq. (1) yields

$$\frac{1}{S_w + 1}\frac{dS_w}{dt} = a_0 u_z - a_2 B_i^* N_i \bar{r}_i - (a_1 B_w N_w \bar{r}_w + a_2 B_i N_i \bar{r}_i) S_w. \quad (9)$$

Here, we denote $a_0 = g(LR_a/c_p R_v T - 1)/R_a T$; $a_1 = 1/q_v + L_w^2/c_p R_v T^2$; $a_2 = 1/q_v + L_w L_i/c_p R_v T^2$.

Integrating Eqs. (3) and (6), and assuming that the size distributions of ice particles and droplets are monodisperse and then substituting $r_w$ and $r_i$ in Eq. (9) results in

$$\frac{1}{S_w + 1}\frac{dS_w}{dt} = a_0 u_z - a_2 N_i \sqrt{r_{i0}^2 + 2cA_i \int_0^t [\xi S_w(t') + \xi - 1]\, dt'} - \left\{ a_1 B_w N_w \sqrt{r_{w0}^2 + 2A_w \int_0^t S_w(t')\, dt'} + a_2 B_i N_i \sqrt{r_{i0}^2 + 2cA_i \int_0^t [\xi S_w(t') + \xi - 1]\, dt'} \right\} S_w. \quad (10)$$

Here, $r_{w0}$ and $r_{i0}$ are droplet and ice particle sizes at the time $t = 0$.

Equation (10) describes supersaturation in a general form in clouds consisting of ice particles and liquid droplets having monodisperse size distribution, and it can be used for estimation of supersaturation in clouds with any phase composition. Some special cases, when analytical solutions can be found, are considered in the following sections.

## 3. Quasi-steady approximation

Assuming that changes in the size of the cloud particles can be neglected so that $\bar{r}_w$ and $\bar{r}_i$ are constant, Eq. (9) yields a solution:

$$S_w = \frac{S_{qsw} - C_0 \exp(-t/\tau_p)}{1 + C_0 \exp(-t/\tau_p)}, \quad (11)$$

where

$$S_{qsw} = \frac{a_0 u_z - b_i^* N_i \bar{r}_i}{b_w N_w \bar{r}_w + b_i N_i \bar{r}_i} \quad (12)$$

is the limiting supersaturation, and

$$\tau_p = \frac{1}{a_0 u_z + b_w N_w \bar{r}_w + (b_i + b_i^*) N_i \bar{r}_i} \quad (13)$$

is the time constant characterizing a time of asymptotical approach of $S_w$ to $S_{qsw}$, that is, at $t/\tau_p \gg 1$, $S_w = S_{qsw}$. Here, $C_0 = (S_{qsw} - S_{w0})/(1 + S_{w0})$; $S_{w0}$ is the supersaturation at $t = 0$; $b_w = a_1 B_w$; $b_i = a_2 B_i$; $b_i^* = a_2 B_i^*$.

The limiting supersaturation $S_{qsw}$ [Eq. (12)] coincides with the solution of Eq. (9), when $dS_w/dt = 0$. Therefore, the physical meaning of $S_{qsw}$ can be interpreted as an *equilibrium* supersaturation; that is, when an increase (decrease) of the relative humidity due to air cooling (heating) is balanced by the depletion (release) of the water vapor by cloud particles. Traditionally, after Squires (1952) and Rogers (1975), the limiting supersaturation $S_{qsw}$ is called *quasi-steady*.[1] We will keep this terminology in the frame of this study. Similarly, the assumption $\bar{r}_w$ = constant and $\bar{r}_i$ = constant in the supersaturation equation (9), will be called *quasi-steady approximation.* Following Mazin (1966, 1968), the constant $\tau_p$ herein will be called *the time of phase relaxation.* The term *integral radius* will be applied to $N_w \bar{r}_w$ and $N_i \bar{r}_i$ following Politovich and Cooper (1988).

The dependence of $q_v$ on supersaturation in the coefficients $a_1$ and $a_2$ has been neglected in Eqs. (1), (9), and (10). The comparison of numerical modeling results (appendix B) with the solution of Eq. (10) shows that for most clouds in the troposphere this assumption works with high accuracy. The solution for Eq. (9) in a more general form, including a dependence of $q_v$ versus $S_w$, is given in appendix C.

## 4. Supersaturation in single-phase clouds

### a. Liquid clouds

Assuming $N_i = 0$, Eq. (10) gives the equation for supersaturation in liquid clouds having a monodisperse droplet size distribution (Korolev 1994):

$$\frac{1}{S_w + 1}\frac{dS_w}{dt} = a_0 u_z - a_1 B_w N_w S_w \sqrt{r_{w0}^2 + 2cA_w \int_0^t S_w(t')\, dt'}. \quad (14)$$

Figure 1 shows solutions of Eq. (14) for different vertical velocities $u_z$. In the ascending parcel, the supersaturation decreases after reaching a maximum (Fig. 1a). The presence of the maximum depends on initial supersaturation $S_w(0)$. If $S_w(0)$ is high enough, $S_w(t)$ will monotonically decrease at all times. It can be shown that for $t \gg \tau_p$ the supersaturation asymptotically ap-

[1] Squires (1952) used the term *quasi-static* for $S_{qsw}$, which has a meaning close to *quasi-steady.*

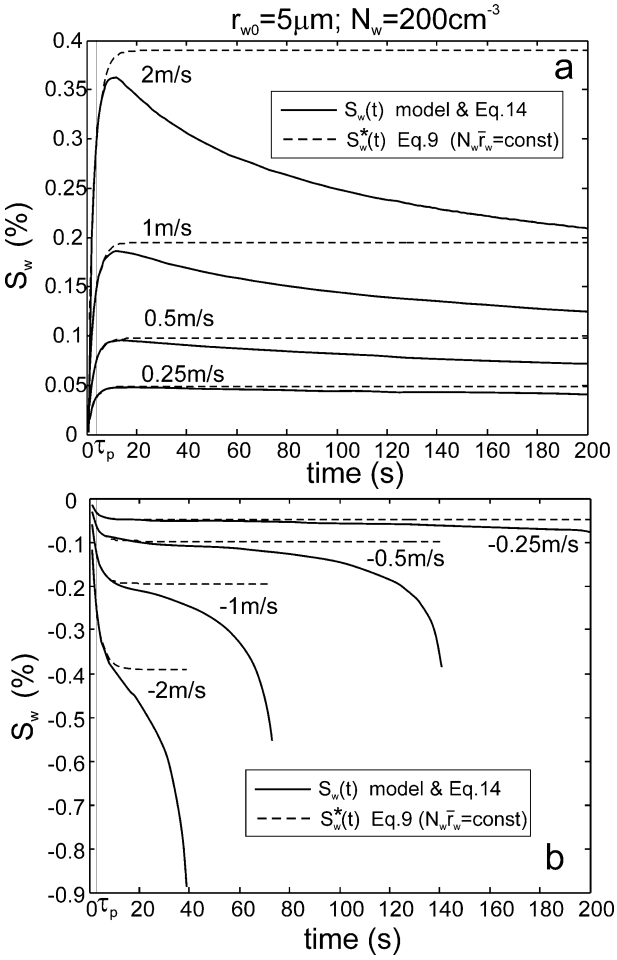


FIG. 1. Changes of supersaturation (solid line) with time in adiabatic (a) ascending and (b) descending liquid cloud parcels containing liquid droplets with $r_{w0} = 5$ $\mu$m and $N_w = 200$ cm$^{-3}$. The solution of Eq. (9) for the quasi-steady approximation ($N_w\bar{r}_w$ = constant and $N_i = 0$) is shown by a dashed line. The time of phase relaxation ($\tau_p = 3.3$ s) is indicated by the vertical line on the left-hand side of (a) and (b). The initial conditions are $S(0) = 0$; $T(0) = 0$°C, $P(0) = 870$ mb.

proaches zero as $S_w(t) \sim t^{-1/3}$ [Sedunov 1974, Eq. (4.3.26) p. 116]. In the descending parcel the supersaturation is negative and decreases monotonically with time to the moment of complete evaporation of droplets (Fig. 1b). After the droplets evaporate the supersaturation changes as $S_w = \exp(-a_0u_zt) - 1$.

Equation (14) gives a rather accurate solution of $S_w$. Comparison shows that the agreement between supersaturation derived from a numerical solution of a system of differential equations Eqs. (B1)–(B7) (appendix B) and that of a single Eq. (14) is better than 1% for a vertical displacement of a few hundred meters. For larger displacements, the deviation between $S_w$ computed from Eq. (14) and Eqs. (B1)–(B7) (appendix B) increases because Eq. (14) does not take into account changes of $a_0$, $a_1$, and $A_w$ with $T$ and $P$.

Dashed lines in Fig. 1 show the solution of Eq. (9)

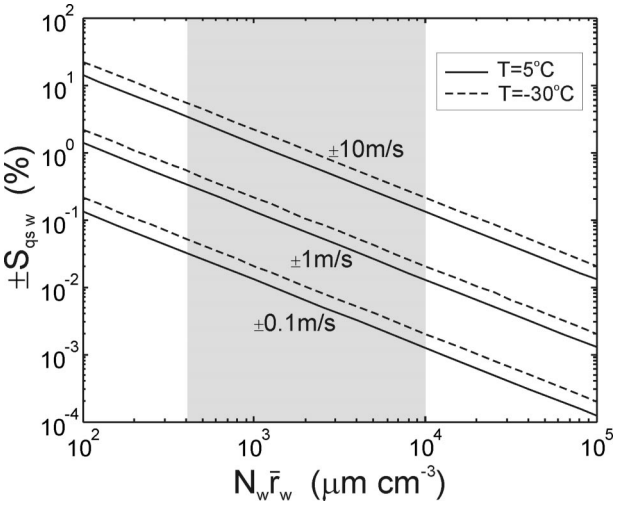


FIG. 2. Quasi-steady supersaturation vs $N_w\bar{r}_w$ in liquid clouds for different vertical velocities ($\pm 0.1$, $\pm 1$, and $\pm 10$ m s$^{-1}$) and different temperatures ($+5°$ and $-30$°C). Gray color indicates $N_w\bar{r}_w$ typical for the liquid clouds in the troposphere; $P = 690$ mb.

for the supersaturation $S^*_w(t)$ for the quasi-steady approximation, that is, when $N_w\bar{r}_w$ = const and $N_i = 0$. As seen from Eq. (14) the quasi-steady approximation can be applied for the time period when

$$r^2_{w0} \gg \left| 2A_w \int_0^t S_w(t')\, dt' \right|. \tag{15}$$

Figure 1 shows that the supersaturation $S_w(t)$ agrees well with $S^*_w(t)$ when $t < \tau_p$. At larger times the difference between $S_w(t)$ and $S^*_w(t)$ increases since condition (15) becomes invalid.

Substituting $N_i = 0$ in Eqs. (12) and (13) gives the expression for quasi-steady supersaturation

$$S_{qsw} = \frac{a_0u_z}{b_wN_w\bar{r}_w} \tag{16}$$

and the time of phase relaxation

$$\tau_p = \frac{1}{a_0u_z + b_wN_w\bar{r}_w}. \tag{17}$$

For characteristic values of $N_w\bar{r}_{w0}$ and $u_z$ typical for liquid clouds, $b_wN_w\bar{r}_w \gg a_0u_z$. Then, neglecting $a_0u_z$ in Eq. (16), gives

$$\tau_p = \frac{1}{b_wN_w\bar{r}_w}. \tag{18}$$

An expression similar to Eq. (16) was originally deduced by Squires (1952). The time of phase relaxation in the form similar to Eq. (18) was first obtained by Squires (1952) and Mazin (1966).

Figure 2 shows $S_{qsw}$ calculated from Eq. (16) for different values of $N_w\bar{r}_w$ and $u_z$. The gray color indicates the range of $N_w\bar{r}_w$ typical for liquid clouds in the troposphere. As seen in Fig. 2 the supersaturation varies

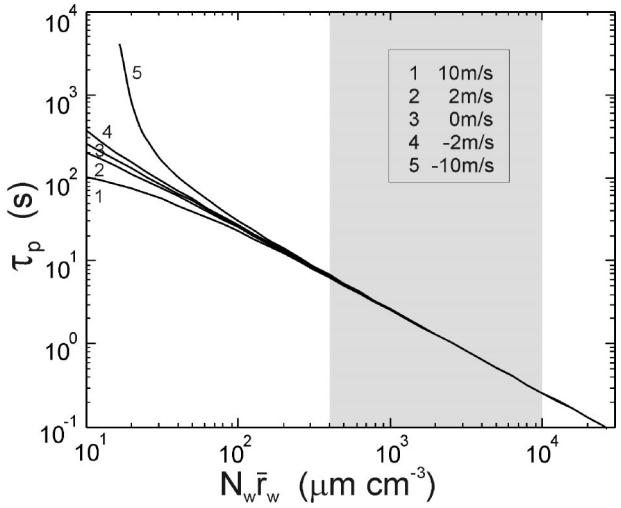


FIG. 3. Time of phase relaxation vs $N_w\bar{r}_w$ in liquid clouds for different vertical velocities. $T = 0$°C, $P = 680$ mb. Gray color indicates $N_w\bar{r}_w$ typical for the liquid clouds in the troposphere.

between $-0.5 < S_w < 0.5\%$ for vertical velocities $-1 < u_z < 1$ m s$^{-1}$. Such vertical velocities would limit the characteristic range of vertical velocity fluctuations in stratiform clouds (Mazin et al. 1984). In convective clouds where the vertical velocities vary in a wider range, for example, $-10 < u_z < 10$ m s$^{-1}$, the supersaturation would experience fluctuations of $-5 < S_w < 5\%$, which is an order of magnitude larger than those in stratiform clouds.

The supersaturation in a vertically moving parcel also depends on temperature and pressure. For fixed $N_w\bar{r}_w$ and $u_z$, the supersaturation increases with decreasing temperature and increasing air pressure (Rogers 1975).

Figure 3 shows the time of phase relaxation versus $N_w\bar{r}_w$ computed from Eq. (17). For typical $N_w\bar{r}_w$, the characteristic time of the phase relaxation in liquid clouds is a few seconds. The effect of vertical velocity $u_z$ becomes significant at small $N_w\bar{r}_w$. However, such a combination of high $u_z$ and low $N_w\bar{r}_w$ is unlikely in liquid clouds. Therefore, the term $a_0u_z$ in the denominator in Eq. (17) can be neglected, and for practical calculations of $\tau_p$ in liquid clouds, Eq. (18) is an accurate approximation.

Equations (9)–(18) neglect the corrections of curvature and salinity of droplets on the rate of droplet growth [Eq. (4)]. Kabanov et al. (1971) showed that the effect of these corrections on $S_{qsw}$ and $\tau_p$ is negligible. Omitting these corrections does not affect our considerations and the final conclusions.

### b. Ice clouds

Similarly to section 2, the equation for supersaturation with respect to ice in glaciated clouds with monodisperse ice particles and $N_w = 0$ can be written as

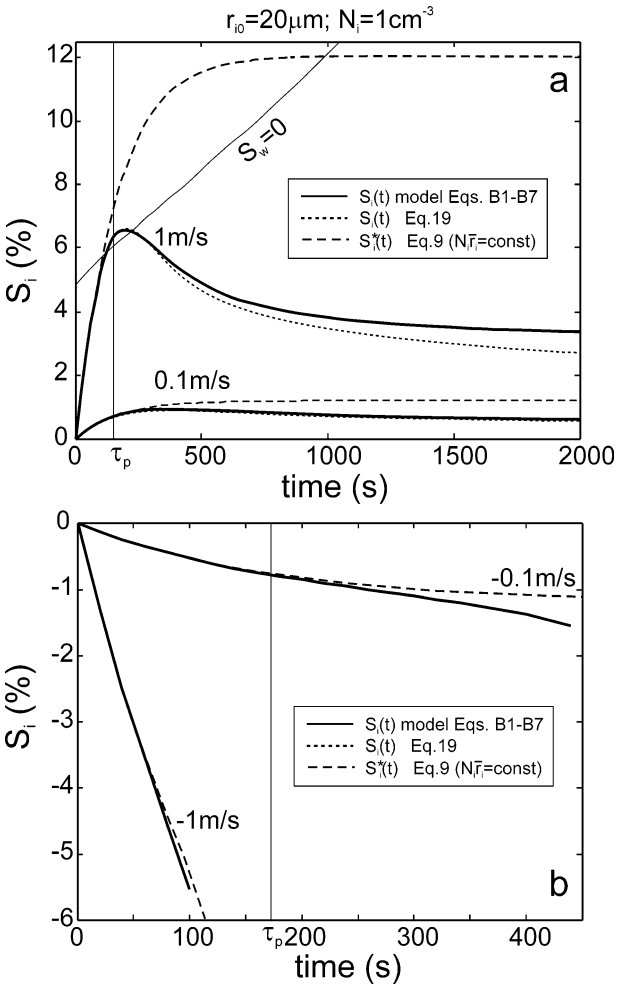


FIG. 4. Changes of supersaturation with time (solid line) in adiabatic (a) ascending and (b) descending ice cloud parcels containing ice particles of $r_{i0} = 20$ $\mu$m and $N_i = 1$ cm$^{-3}$. The solution of Eq. (9) for the quasi-steady approximation ($N_i\bar{r}_i$ = constant and $N_w = 0$) is shown by a dashed line. In (a), line $S_w = 0$ corresponds to saturation over water at $u_z = 1$ m s$^{-1}$. The vertical lines indicate the initial values of time of phase relaxation: (a) $\tau_p = 168$ s, ($u_z = 0.1$ m s$^{-1}$), $\tau_p = 152$ s ($u_z = 1$ m s$^{-1}$, not shown); (b) $\tau_p = 173$ s ($u_z = -0.1$ m s$^{-1}$), $\tau_p = 193$ s ($u_z = -1$ m s$^{-1}$, not shown). The initial conditions are $S_i(0) = 0$, $T(0) = -5$°C, and $P(0) = 870$ mb.

$$\frac{1}{S_i + 1}\frac{dS_i}{dt} = a_0u_z - a_3B_{i0}N_iS_i\sqrt{r_{i0}^2 + 2cA_i\int_0^t S_i(t')\,dt'}. \quad (19)$$

Here, $a_3 = 1/q_v + L_i^2/c_pR_vT^2$; $B_{i0} = 4\pi\rho_i cA_i/\rho_a$.

Figure 4 shows changes of supersaturation $S_i(t)$ in ice cloud with $r_{i0} = 20$ $\mu$m and $N_i = 1$ cm$^{-3}$ for different vertical velocities. The ascending parcel takes longer to reach maximum supersaturation in glaciated cloud than in liquid clouds because of lower values of $N_i\bar{r}_i$ compared to $N_w\bar{r}_w$. Dashed lines show the supersaturation $S_i^*(t)$ resulted from the solution of Eq. (19) for the quasi-

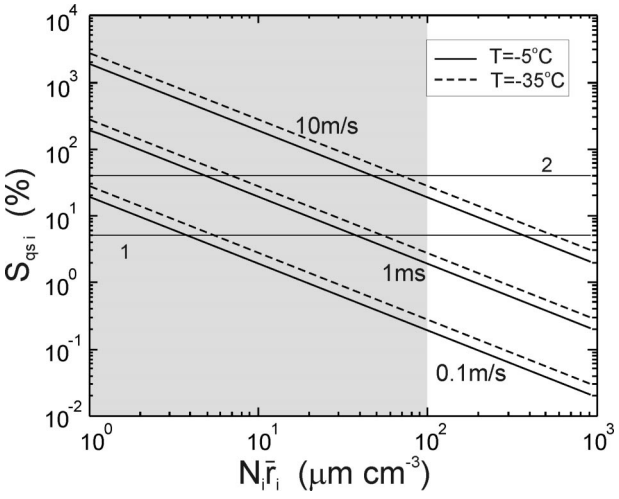


FIG. 5. Quasi-steady supersaturation vs $N_i\bar{r}_i$ in ice clouds for different vertical velocities. Horizontal lines indicate saturation over water at −5°C (line 1); and at −35°C (line 2). $P$ = 870 mb. Gray color indicates $N_i\bar{r}_i$ typical for the ice clouds.

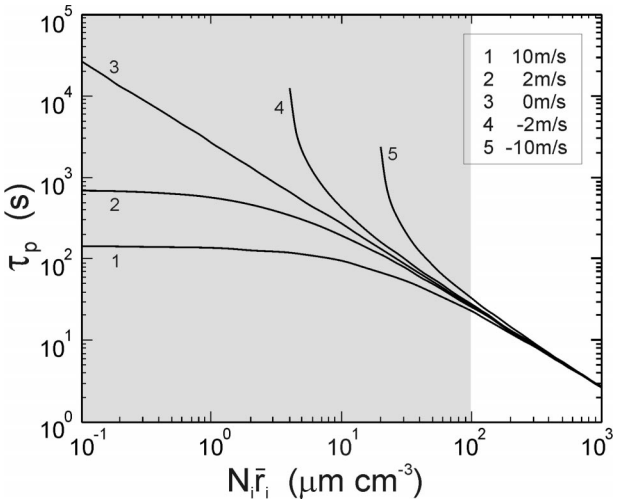


FIG. 6. Time of phase relaxation vs $N_i\bar{r}_i$ in ice clouds for different vertical velocities; $T$ = −10°C; $P$ = 680 mb. Gray color indicates $N_i\bar{r}_i$ typical for the ice clouds.

steady approximation, that is, when $N_i\bar{r}_i$ = const. The difference between $S_i(t)$ and $S_i^*(t)$ is also typically larger in glaciated clouds than in liquid clouds.

The supersaturation in Eq. (9) was considered with respect to water. Similarly, this equation can be rewritten for the supersaturation with respect to ice. The solution of this equation yields the quasi-steady supersaturation

$$S_{qsi} = \frac{a_0 u_z}{b_{i0} N_i \bar{r}_i} \tag{20}$$

and the time of phase relaxation

$$\tau_p = \frac{1}{a_0 u_z + b_{i0} N_i \bar{r}_i}, \tag{21}$$

where $b_{i0} = a_3 B_{i0}$.

Figure 5 shows $S_{qsi}$ calculated from Eq. (20) for different values of $N_i\bar{r}_i$ and $u_z$. In situ measurements showed that the average concentration of ice particles in glaciated clouds is 2–5 cm$^{-3}$ with a characteristic size between 25–40 $\mu$m in the temperature range $-35° < T < 0$°C (Korolev et al. 2003). Due to lower values of $N_i\bar{r}_i$, the supersaturation $S_{qsi}$ in glaciated clouds may be significantly higher compared to $S_{qsw}$ in liquid clouds. As seen from Fig. 5 for $u_z$ = 1 m s$^{-1}$ and for typical $N_i\bar{r}_i$, the supersaturation $S_{qsi}$ may range from a few to hundreds of percent with respect to ice. However, such a high supersaturation will never be reached in clouds at $T > -40$°C, since an increase of the supersaturation is limited by the saturation over water. Lines 1 and 2 in Fig. 5 show the saturation over water for −5° and −35°C, respectively. As soon as the saturation with respect to water is exceeded, the activation of cloud condensation nuclei (CCN), which always exist in the troposphere in large numbers, will occur. The activation of newly formed droplets will result in rapid depletion of the water vapor and prevent continuous increase of the supersaturation, keeping the water vapor pressure close to the saturation over water.

Figure 6 shows the time of phase relaxation calculated from Eq. (21). For typical $N_i\bar{r}_i$ in ice clouds the characteristic time of the phase relaxation may vary from a few minutes to a few hours. Comparing diagrams in Figs. 3 and 6, it can be concluded that the processes related to changes in water vapor due to evaporation or condensation of ice particles in the glaciated clouds are on average slower than those related to liquid droplets. In other words the ''condensational'' activity of droplets in tropospheric clouds is typically higher than that of ice particles due to on average lower values of integral radius of the ice particles than those of the liquid droplets. The effect of $u_z$ on $\tau_p$ is more pronounced in ice clouds compared to liquid ones.

The ice particles in this section were treated as ice spheres having the capacitance $c$ = 1. Because for the majority of ice particles $c < 1$, the coefficients $B_i$ and $B_i^*$ will be reduced. This would result in supersaturation and time of phase relaxation values higher than those shown in Figs. 4 and 5. Therefore, the values of $S_i$, $S_{qsi}$ and $\tau_p$ should be considered as lower estimates.

## 5. Supersaturation in mixed-phase clouds

Cloud droplets may stay in a metastable liquid condition down to about −40°C. This results in a population of cloud particles below 0°C that may consist of a mixture of ice particles and liquid droplets. Such clouds are usually called ''mixed-phase'' or ''mixed'' clouds. Due to the difference of water vapor saturation over ice and liquid, the mix of ice particles and liquid droplets is condensationally unstable and may exist only for a limited time. The behavior of supersaturation in mixed-

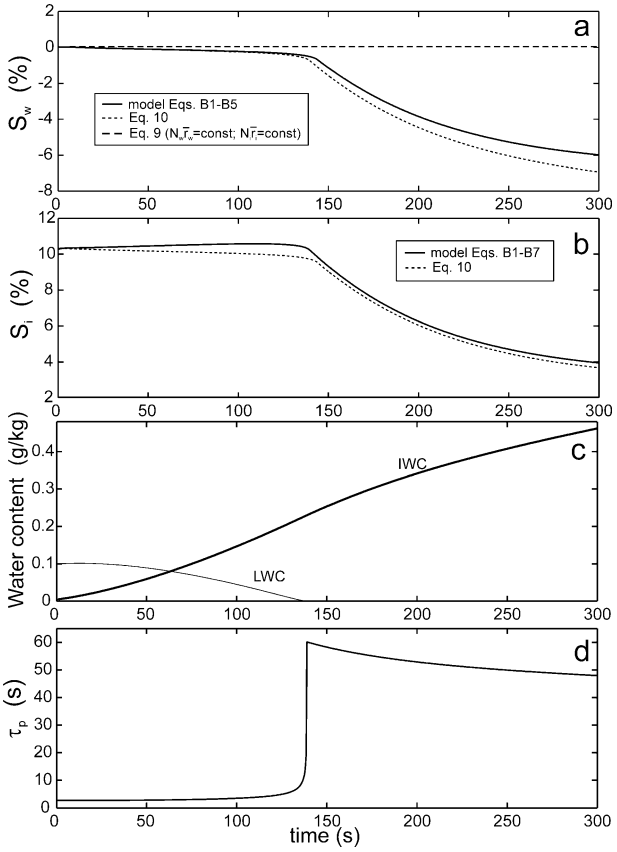


FIG. 7. Time history of (a) $S_w$, (b) $S_i$, (c) LWC and IWC, and (d) $\tau$ in an ascending mixed-phase parcel; $T(0) = -10°C$, $P(0) = 680$ mb, $S_w(0) = 0$, $N_i = 1$ cm$^{-3}$, $r_i(0) = 10$ $\mu$m, LWC(0) = 0.1 g kg$^{-1}$, $N_w = 200$ cm$^{-3}$, $u_z = 0.8$ m s$^{-1}$.

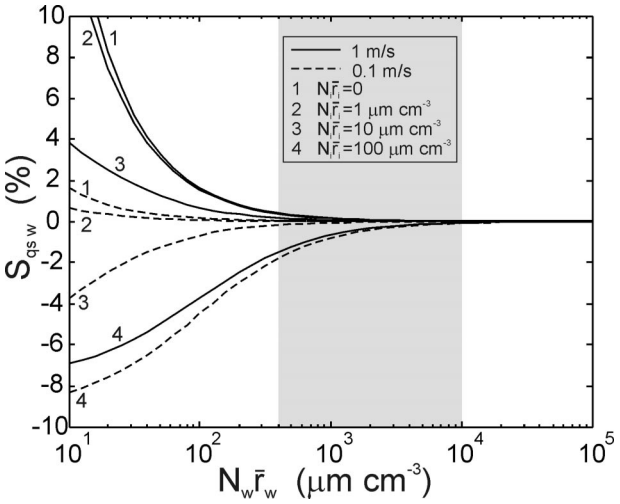


FIG. 8. Quasi-steady supersaturation vs $N_w\bar{r}_w$ in mixed-phase clouds for different $N_i\bar{r}_i$ and two vertical velocities: 0.1 m s$^{-1}$ (dashed line) and 1 m s$^{-1}$ (solid line); $T = -10°C$, $P = 680$ mb. Gray color indicates $N_w\bar{r}_w$ typical for liquid and mixed phase clouds in the troposphere.

phase clouds is more complex compared to that in single-phase liquid or ice clouds. Since the saturating water vapor pressure over ice is less than that over water, there are several possible scenarios for the evolution of the three-phase colloidal system. Depending on the values of $u_z$, $P$, $T$, $N_i$, $\bar{r}_i$, $N_w$, and $\bar{r}_w$, the liquid and ice particles may (a) both grow or (b) both evaporate or (c) ice particles may grow while liquid droplets evaporate. The last process, when the ice particles grow at the expense of evaporating droplets, is known as the Wegener–Bergeron–Findeisen (WBF) mechanism (Wegener 1911; Bergeron 1935; Findeisen 1938).

Figure 7 shows time histories of $S_w$, $S_i$, liquid water content (LWC), ice water content (IWC), and $\tau_p$ in a cloud parcel ascending with $u_z = 0.8$ m s$^{-1}$. The time of phase relaxation $\tau_p$ was calculated for current values of $r_w(t)$, $r_i(t)$, $e(t)$, $T(t)$, and $P(t)$. During the first 15 s or so, both droplets and ice particles are growing. During this period of time the ice particles deplete water vapor at a higher rate compared to the liquid droplets, eventually reducing $S_w$ to below zero. As a result, the droplets start to evaporate, whereas the ice particles keep growing. After 140 s the droplets completely evaporate and the cloud becomes glaciated. After the moment of glaciation the time of phase relaxation $\tau_p$ jumps up (Fig. 7d), and the supersaturation $S_w$ decreases toward the value equivalent to the saturation over ice, while $S_i$ decreases toward zero.

Dotted lines in Figs. 7a,b show solutions for $S_w$ and $S_i$ calculated from Eq. (10). The solution of Eq. (10) gives a reasonable agreement with that of (B1)–(B7).

Figure 8 shows quasi-steady supersaturation in mixed-phase clouds as a function of $N_w\bar{r}_w$ for different $N_i\bar{r}_i$ for two updraft velocities 0.1 and 1 m s$^{-1}$. The supersaturation $S_w$ in the ascending mixed-phase cloud may be either positive or negative. The sign of the supersaturation is related to the balance between the rate of supersaturation growth due to adiabatic cooling and the rate of water vapor depletion by ice particles and depletion or supply by liquid droplets. For example, if $N_i\bar{r}_i$ is high enough then the ice particles will absorb water vapor rapidly reducing it to saturation over ice. If $N_i\bar{r}_i$ is too low, then ice particles will play no significant role in the water vapor depletion, and the supersaturation will be controlled mainly by liquid droplets.

Figure 9 shows the time of phase relaxation in mixed-phase clouds for $u_z = 0$. In the mixed phase clouds with typical $N_w\bar{r}_w$ (Korolev et al. 2003), the ice particles do not affect the time of phase relaxation until $N_i\bar{r}_i$ reaches values above 100 $\mu$m cm$^{-3}$. This means that, for such mixed-phase clouds, the time of phase relaxation is mainly defined by liquid droplets. At the final stage of cloud glaciation due to the WBF mechanism, when $N_w\bar{r}_w$ becomes small, $\tau_p$ is mainly defined by ice particles.

In mixed-phase clouds, the droplets would stay in equilibrium (i.e., they will neither grow nor evaporate) if $S_w = 0$. The ice particles under this condition will

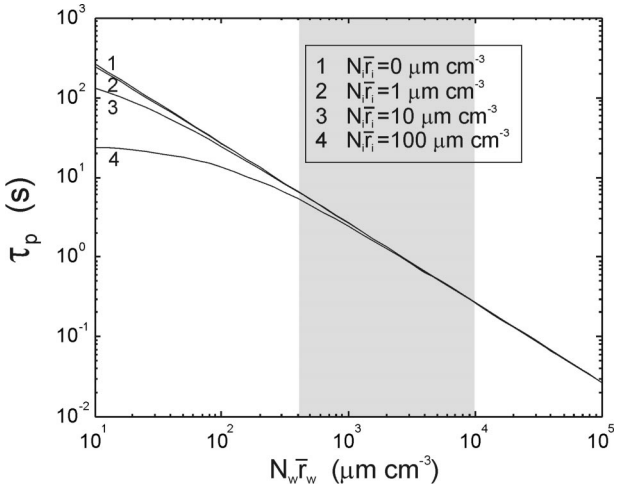


FIG. 9. Time of phase relaxation vs $N_w\bar{r}_w$ in mixed-phase clouds for different $N_i\bar{r}_i$; $T = -10$°C, $P = 680$ mb. Gray color indicates $N_w\,\bar{r}_w$ typical for the liquid and mixed phase clouds in the troposphere.

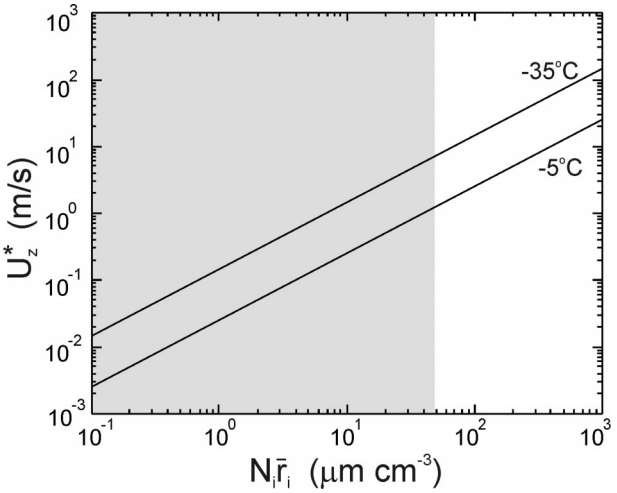


FIG. 10. Threshold vertical velocity such that, in a mixed-phase cloud at $u_z > u_z^*$, both droplets and ice particles grow. Calculations were done for temperatures −5° and −35°C; $P = 680$ mb. Gray color indicates $N_i\bar{r}_i$ typical for the mixed phase and ice clouds.

keep growing because $S_i > 0$. Substituting $S_{qsw} = 0$ in Eq. (12) yields a threshold velocity of ascent when droplets remain in equilibrium:

$$u_z^* = \frac{b_i^* N_i \bar{r}_i}{a_0}. \tag{22}$$

Substituting Eq. (7) in (12) and assuming $S_i = 0$ yields a condition for the equilibrium of ice particles; that is, ice particles neither grow nor evaporate:

$$u_z^o = \frac{(1 - \xi) b_w N_w \bar{r}_w}{\xi a_0}. \tag{23}$$

Thus, if $u_z > u_z^*$, both droplets and ice particles grow; if $u_z^0 < u_z < u_z^*$, the droplets evaporate, whereas the ice particle grow; if $u_z < u_z^0$, both droplets and ice particles evaporate.

The velocity $u_z^*$ may also be considered as a threshold velocity for the activation of liquid droplets in ice clouds when $u_z > u_z^*$. Basically, Eq. (22) defines a condition for maintaining a mixed-phase in a cloud. It is worth noting that the threshold velocity $u_z^*$ does not depend on $N_w\bar{r}_w$, and $u_z^0$ does not depend on $N_i\bar{r}_i$.

Figure 10 shows the dependence of the threshold velocity $u_z^*$ versus $N_i\bar{r}_i$. The velocity $u_z^*$ does not exceed a few meters per second for typical values of $N_i\bar{r}_i$ (Fig. 10). Such vertical velocities can be generated by turbulence in stratiform clouds or regular convective motions in cumulus clouds. This results in an important conclusion that liquid droplets may be easily activated in ice clouds under relatively small vertical velocities having turbulent or regular nature keeping the cloud in mixed-phase condition. It should be noted that $u_z^*$ was calculated for spherical ice particles, that is, $c = 1$, whereas usually for natural ice particles $c < 1$. Because $u_z^*$ is linearly related to $c$ [Eq. (22)], the actual $u_z^*$ would be lower than that calculated above, and $u_z^*$ in Fig. 10 should be scaled down by a factor of $c$. Therefore, $u_z^*$ shown in Fig. 10 should be considered an upper estimate.

An example when an ice cloud may transfer into a mixed one is shown in Fig. 4a for the parcel ascending at $u_z = 1$ m s$^{-1}$. The relative humidity in the parcel exceeds saturation over water (curve $S_w = 0$) between 140 and 210 s. Liquid droplets will be activated during this period and the ice cloud will turn into a mixed cloud. The study of Korolev and Isaac (2003) showed that periodic oscillations of vertical velocity may result in a periodic activation and evaporation of liquid droplets in ice clouds. The most interesting part of this process is that the periodic activation and evaporation of droplets in ice clouds under such oscillations are not limited in time and may occur over an infinitesimally long period.

Figure 11 shows a diagram of $u_z^0$ versus $N_w\bar{r}_w$. The evaporation of both droplets and ice particles may occur only in downdrafts. For typical $N_w\bar{r}_w$ the values of $u_z^0$ are unrealistically high. In practice the simultaneous evaporation of droplets and ice particles may occur only during the final stages of cloud glaciation, when $N_w\bar{r}_w$ becomes small.

## 6. Glaciating time of mixed-phase clouds

Based on Eq. (12) in the absence of a vertical velocity ($u_z = 0$), the supersaturation over water in a mixed-phase cloud is always negative:

$$S_{qsw} = -\frac{b_i^* N_i \bar{r}_i}{b_w N_w \bar{r}_w + b_i N_i \bar{r}_i}. \tag{24}$$

As seen from Fig. 12, for the case $u_z = 0$ for typical $N_i\bar{r}_i$ and $N_w\bar{r}_w$, the supersaturation in mixed-phase clouds is close to zero ($|S_{qsw}| < 1\%$). It means that in mixed-phase clouds the evaporating droplets tend to

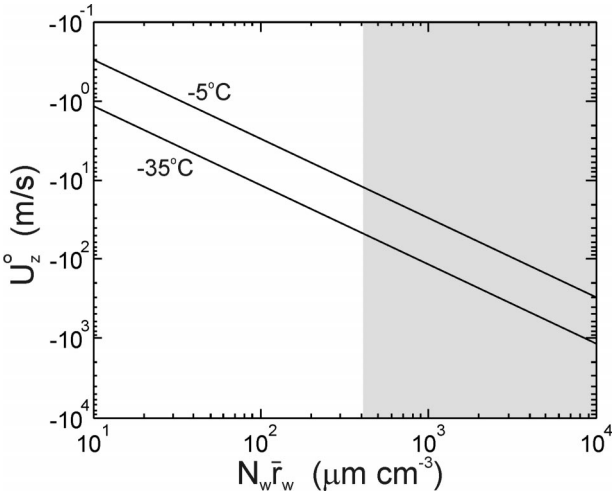


FIG. 11. Threshold vertical velocity such that, in a mixed-phase cloud at $u_z < u_z^0$, both droplets and ice particles evaporate. Calculations were done for temperatures −5° and −35°C; $P$ = 680 mb. Gray color indicates $N_w\bar{r}_w$ typical for the liquid and mixed phase clouds in the troposphere.

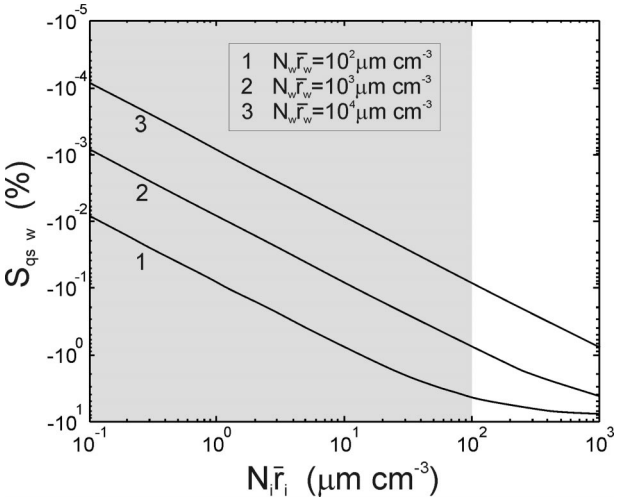


FIG. 12. Quasi-steady supersaturation in mixed-phase cloud for $u_z = 0$ for different $N_w\bar{r}_w$; $T = -10$°C, $P$ = 680 mb. Gray color indicates $N_i\bar{r}_i$ typical for the mixed phase and ice clouds.

maintain the water vapor pressure close to saturation over water. This creates a basis for the analytical estimation of the time of glaciation in mixed-phase clouds. The purpose of the following section is to consider the glaciating time of mixed-phase clouds at $u_z = 0$ solely due to the WBF mechanism.

Consider an adiabatic parcel containing a mixture of liquid droplets and ice particles. As in section 2, assume that the concentration of droplets and ice particles stay constant, and no nucleation of ice particles occur. The mass growth of an individual ice particle can be written as

$$\frac{dm_i}{dt} = 4\pi\rho_i c A_i r_i S_i. \tag{25}$$

Because the water vapor pressure in mixed-phase clouds is close to the saturation over water, the supersaturation in mixed-phase clouds can be estimated as $S_i = [E_w(T) - E_i(T)]/E_i(T)$. Therefore, the ice particles are growing at the expense of liquid droplets only, and at the moment of glaciation ($\tau_{gl}$), the mass of all ice particles will be approximately

$$W_i(\tau_{gl}) = W_i(t_0) + W_w(t_0). \tag{26}$$

Here, $W_i(t_0)$ and $W_w(t_0)$ are initial ice and liquid water content, respectively. Assuming that the ice particles are monodisperse, the individual ice particle mass at the initial moment of time $t_0 = 0$ is

$$m_i(t_0) = \frac{W_i(t_0)}{N_i}. \tag{27}$$

Because the number concentration of the ice particles $N_i$ stays constant, the mass of a single ice particle at the moment of glaciation will be

$$m_i(\tau_{gl}) = \frac{W_i(\tau_{gl})}{N_i} = \frac{W_i(t_0) + W_w(t_0)}{N_i}. \tag{28}$$

Integrating Eq. (25) from $m_i(t_0)$ to $m_i(\tau_{gl})$, and substituting Eqs. (27) and (28), yields the glaciation time

$$\tau_{gl} = \frac{1}{4\pi c A_i S_i}\left(\frac{9\pi\rho_i}{2}\right)^{1/3}\left\{\left[\frac{W_w(t_0) + W_i(t_0)}{N_i}\right]^{2/3} - \left[\frac{W_i(t_0)}{N_i}\right]^{2/3}\right\}. \tag{29}$$

If $W_w(t_0) \gg W_i(t_0)$, then Eq. (29) will be simplified (Mazin 1983):

$$\tau_{gl} = \frac{1}{4\pi c A_i S_i}\left(\frac{9\pi\rho_i}{2}\right)^{1/3}\left[\frac{W_w(t_0)}{N_i}\right]^{2/3}. \tag{30}$$

Equation (29) indicates that to a first approximation the time of glaciation is insensitive to the size spectra of liquid droplets and depends only on ice particles number concentration and the initial LWC and IWC. Figure 13 shows the dependence of $\tau_{gl}$ versus $T$ for different $N_i$ calculated from a numerical model (appendix B), and that derived from Eq. (29). The calculations were done for $W_{w0}$ = 0.1 g m$^{-3}$ and $P$ = 680 mb. As seen from Fig. 13, $\tau_{gl}$ has a minimum around −12°C, where the difference between the saturation vapor pressure over water and ice has a maximum. The glaciation time increases toward 0°C and cold temperatures, where the difference $E_w(T) - E_i(T)$, and therefore $S_i$, approaches zero.

The glaciation time derived from Eq. (29) agrees well with that calculated from the numerical model for ice concentrations less 1 cm$^{-3}$. The difference between $\tau_{gl}$ calculated from the numerical model and Eq. (29) increases with an increase of $N_i$ (Fig. 13). For example,

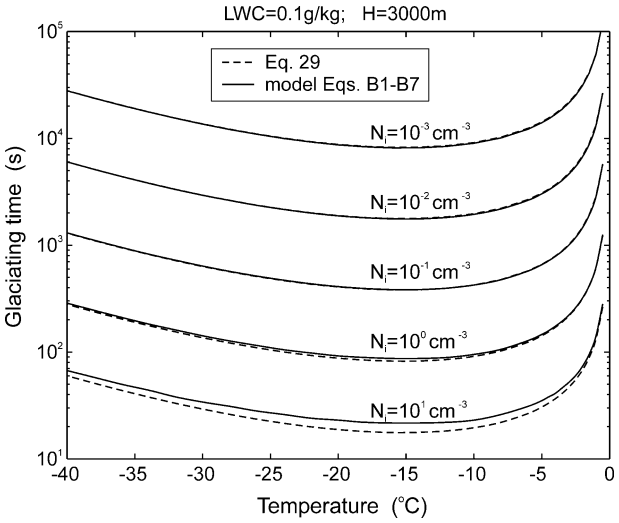


FIG. 13. Time of glaciation of a mixed-phase cloud vs temperature for $u_z = 0$; $\mathrm{LWC}_0 = 0.1$ g kg$^{-1}$; $T = -15$°C; $P = 680$ mb.

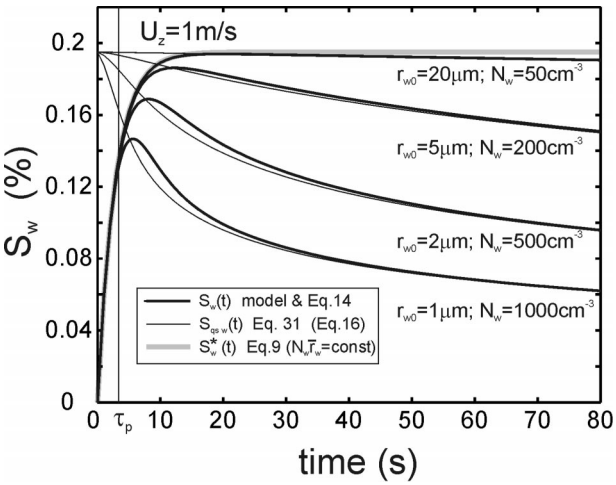


FIG. 14. Comparison of the supersaturation $S_w(t)$, $S_{\mathrm{qsw}}(t)$, and $S^*_w(t)$ in ascending liquid clouds having the same $N_w\overline{r}_w = 1000$ $\mu$m cm$^{-3}$, but different $N_w$ and $\overline{r}_{w0}$; $u_z = 1$ m s$^{-1}$; $T(0) = 0$°C; $P(0) = 870$ mb. Gray line $S^*_w(t)$ is the solution of Eq. (9) for the quasi-steady approximation ($N_w\overline{r}_w$ = constant and $N_i = 0$).

for $N_i = 10$ cm$^{-3}$ and $N_i = 1$ cm$^{-3}$ the relative difference at $T = -15$°C reaches about 40% and 5%, respectively. For ice particle concentrations less than $N_i = 10^{-1}$ cm$^{-3}$, the maximum relative error between the model and Eq. (29) does not exceed 1%. Therefore, Eqs. (29) and (30) can be used as an estimate of $\tau_{\mathrm{gl}}$. The agreement between Eq. (29) and the numerical model indicates that, in mixed-phase clouds, the vapor pressure is close to saturation over liquid water, and the rate of decrease of LWC is equal to the rate of growth of IWC.

For nonspherical particles, the glaciating time should be scaled up by a factor of $c^{-1}$ according to Eq. (29). In real clouds, the glaciating time can be reduced compared to Eq. (29) due to ice multiplication and freezing of droplets, or increased due to sedimentation and aggregation. Glaciation due to the WBF mechanism in vertically ascending and descending mixed-phase cloud parcels was considered in detail by Korolev and Isaac (2003).

## 7. Relation between $S$ and $S_{\mathrm{qs}}$

In situ measurements of supersaturation in clouds is a great challenge. At present, there are no aircraft instruments providing measurements of the supersaturation. Our knowledge about the in-cloud supersaturation is based mainly on numerical modeling. Another approach was used in studies by Warner (1968), Paluch and Knight (1984), and Politovich and Cooper (1988). They have estimated the supersaturation in liquid clouds from Eq. (16) based on in situ measurements of $u_z$ and $N_w\overline{r}_w$. It was considered that ''supersaturation can be computed using a quasi-steady assumption that the condensation rate just balances the tendency for supersaturation to increase during ascent'' (Paluch and Knight 1984). However, as seen in Fig. 1, such a balance may only be reached at the point where $S_w(t)$ has a maximum; that is, $dS_w/dt = 0$. Politovich and Cooper (1988) stated that ''the value of $S$ may be assumed near its quasi-steady value when the contributions to the temporal variations of $S_{\mathrm{qs}}$ from frequencies $> \tau_p^{-1}$ are negligible.''

So far it is not clear how accurate the estimate of $S_w$ from $S_{\mathrm{qsw}}$ calculated from measurements of $u_z$ and $N_w\overline{r}_w$ is. The difference between $S_w$ and $S_{\mathrm{qsw}}$ can be found by substituting the current values of $r_w(t)$, $N_w(t)$,[2] $e(t)$ $T(t)$, and $P(t)$ calculated from a numerical model (appendix B) into the expression for the quasi-steady approximation [Eq. (16)]:

$$S_{\mathrm{qsw}}(t) = \frac{a_0(t)u_z}{b_w(t)N_w(t)\overline{r}_w(t)} = \frac{a_0(t)u_z}{b_w(t)N_w(t)\sqrt{r_{0w}^2 + 2A_w(t)\int_0^t S_w(t')\,dt'}}. \quad (31)$$

A remarkable property of $S_{\mathrm{qsw}}(t)$ is that it approaches $S_w(t)$ asymptotically over time when $u_z$ = constant; that is,

$$\lim_{i\to\infty}\left[\frac{S_{\mathrm{qsw}}(t)}{S_w(t)}\right] = 1. \quad (32)$$

A rigorous mathematical proof of Eq. (32) is not trivial and it goes beyond the scope of this paper. Numerical modeling indicates that Eq. (32) is valid both for liquid, ice and mixed clouds. Some examples are shown in Figs. 14, 15, and 16. The difference between $S_{\mathrm{qsw}}(t)$ and $S_w(t)$

[2] Note, that the concentration $N_w$ changes with time, due to changes of the air density $\rho_a$. However, the concentration $n_w = N_w/\rho_a$ stays constant.

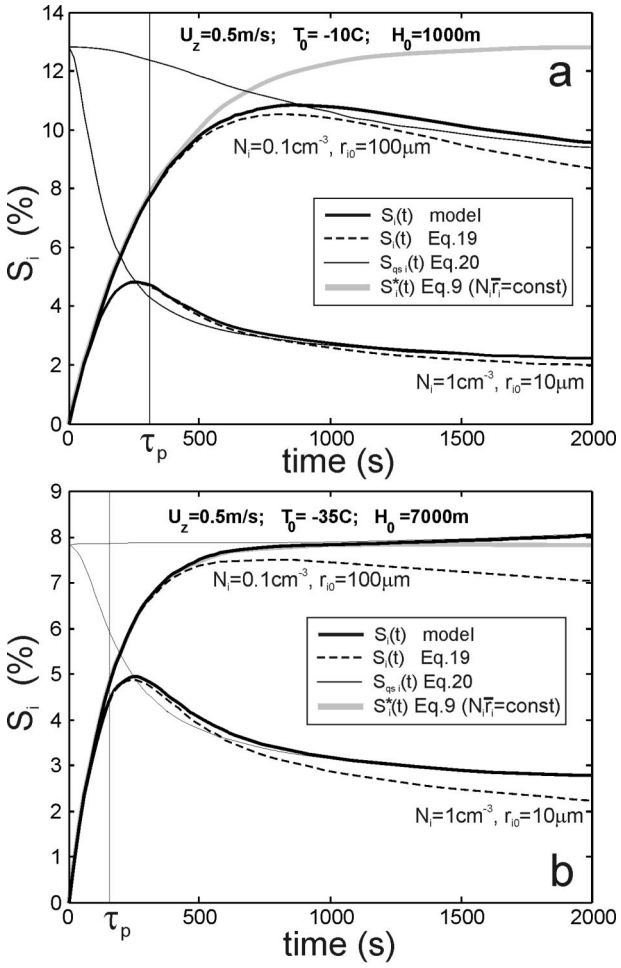


FIG. 15. Comparison of the supersaturation $S_i(t)$, $S_{qsi}(t)$, and $S_i^*(t)$ in ascending ice clouds having the same $N_i\bar{r}_i = 10$ $\mu$m cm$^{-3}$, but different $N_i$ and $\bar{r}_{i0}$; $u_z = 0.5$ m s$^{-1}$; (a) $T(0) = -10$°C; $P(0) = 870$ mb, (b) $T(0) = -35$°C, $P(0) = 360$ mb. Thin line $S_{qsi}(t)$ is the quasi-steady supersaturation calculated from Eq. (20) for current $r_i(t)$, $N_i(t)$, $e(t)$, $T(t)$, and $P(t)$. Gray line $S_i^*(t)$ is the solution of Eq. (9) calculated with respect to ice for the quasi-steady approximation ($N_i\bar{r}_i$ = constant and $N_w = 0$).

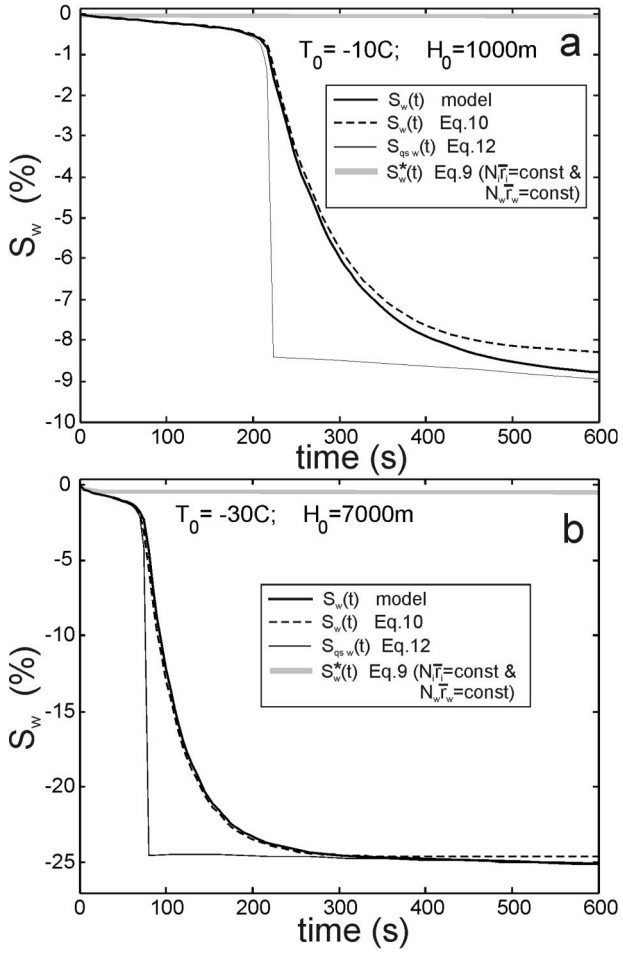


FIG. 16. Comparison of the supersaturation $S_w(t)$, $S_{qsw}(t)$ and $S_w^*(t)$ in ascending mixed-phase clouds; $N_w = 200$ cm$^{-3}$, LWC(0) = 0.2 g m$^{-3}$, $N_i = 1$ cm$^{-3}$, $\bar{r}_{i0} = 10$ $\mu$m, $u_z = 0.25$ m s$^{-1}$; (a) $T(0) = -10$°C; $P(0) = 870$ mb; (b) $T(0) = -30$°C, $P(0) = 360$ mb. Thin line $S_{qsw}(t)$ is the quasi-steady supersaturation calculated from Eq. (12) for current $r_w(t)$, $N_w(t)$, $r_i(t)$, $N_i(t)$, $e(t)$, $T(t)$, and $P(t)$. Gray line $S_w^*(t)$ is the solution of Eq. (9) for the quasi-steady approximation ($N_w\bar{r}_w$ = constant and $N_i\bar{r}_i$ = constant).

[or $S_{qsi}(t)$ and $S_i(t)$] becomes less than 10% usually within a characteristic time $3\tau_p$ depending on $N_w$, $\bar{r}_{w0}$, $u_z$ and initial $S(0)$, $T(0)$, and $P(0)$. Under some conditions, the 10% agreement between $S_{qsw}(t)$ and $S_w(t)$ can be reached during a time period less than $\tau_p$. For example in Fig. 14, for the case with $N_w = 50$ cm$^{-3}$, $\bar{r}_{w0} = 20\mu$m, and $S_w(0) = 0$, the ratio $\Delta S_w/S_w = (S_{qsw} - S_w)/S_w$ becomes less than 10% after about $3\tau_p$ ($\sim$10 s), for $N_w = 1000$ cm$^{-3}$ and $\bar{r}_{w0} = 1$ $\mu m$ the ratio $\Delta S_w/S_w$ reaches 10% difference after $1.5\tau_p$ ($\sim$5 s). Note that $N_w\bar{r}_w$ is the same for both cases.

The behavior of $S_{qsi}(t)$ in glaciated clouds is similar to that in liquid clouds (Fig. 15). The characteristic time of approach of $S_{qsi}(t)$ to $S_i$ is about two orders of magnitude higher than in liquid clouds for typical $N_w\bar{r}_w$ and $N_i\bar{r}_i$. For the cases shown in Fig. 15 this time ranges from about 200 to 800 s. In high-altitude clouds (Fig. 15b, $H = 7000$ m, $T = -35$°C) the ice particles accommodate the water vapor excess faster than that in low-level clouds (Fig. 15a, $H = 1000$ m, $T = -10$°C).

Figure 16 shows changes of the supersaturation in two identical mixed clouds at two altitudes. The supersaturation of mixed-phase clouds changes in a step-wise manner (Fig. 16). Before droplet evaporation the supersaturation $S_w$ is close to zero, which is in agreement with the discussion in section 5. After complete droplet evaporation, $S_{qsw}(t)$ drops to the value equivalent to the saturation over ice, whereas $S_w(t)$ gradually approaches the same value. It is worth noting that glaciation occurs faster in high-altitude clouds (Fig. 16b) compared to that in low-level clouds (Fig. 16a).

## 8. Discussion

In this section we will formulate and discuss the limiting conditions for the quasi-steady approximation. The time of phase relaxation $\tau_p$ is the characteristic timescale of changing of $S_{qsw}$. Therefore, the characteristic time of changes of different coefficients and parameters, considered as constant, should be much larger than $\tau_p$ (Kabanov et al. 1971). For the following estimations it will be assumed that pressure and temperature change from 1000 to 300 mb, and from 0° to −40°C, respectively; for liquid clouds $\tau_p \sim$ 1–10 s, $|u_z| = 0.1$–10 m s$^{-1}$; for ice clouds $\tau_p \sim 10^2$–$10^3$ s, $|u_z| = 0.1$–1 m s$^{-1}$.

### a. Changes of pressure and temperature

The following limitation should be imposed on the changes of pressure and temperature in the frame of the quasi-steady approximation:

$$\left|\frac{\Delta P}{\Delta t}\right| \ll \frac{P}{\tau_p} \tag{33}$$

$$\left|\frac{\Delta T}{\Delta t}\right| \ll \frac{T}{\tau_p}. \tag{34}$$

Using the hydrostatic approximation [Eq. (A9)] for liquid clouds $|dp/dt| \sim 10^0$–$10^2$ N m$^{-2}$ s$^{-1}$, and for ice clouds $|dp/dt| \sim 10^0$–$10^1$ N m$^{-2}$ s$^{-1}$. The characteristic values of $P/\tau_p$ in liquid and ice clouds are $10^4$–$10^5$ N m$^{-2}$ s$^{-1}$ and $10^2$–$10^3$ N m$^{-2}$ s$^{-1}$, respectively.

In liquid clouds $|dT/dt| < \gamma_a u_z \sim 10^{-1}$–$10^{-3}$ K s$^{-1}$ and in ice clouds $|dT/dt| < \sim 10^{-2}$–$10^{-3}$ K s$^{-1}$. The characteristic values of $T/\tau_p$ in liquid and ice clouds are $10^1$–$10^2$ K s$^{-1}$, and $10^{-1}$–$10^0$ K s$^{-1}$.

Therefore, the conditions (33) and (34) are satisfied both in liquid and ice clouds.

### b. Changes of particle concentration

The changes of the cloud particle concentration in the quasi-steady approximation will be limited by the condition

$$\left|\frac{\Delta N}{\Delta t}\right| \ll \frac{N}{\tau_p}. \tag{35}$$

In liquid and mixed clouds the characteristic values of $N_w/\tau_p \sim 10^0$–$10^3$ cm$^{-3}$ s$^{-1}$, in ice clouds $N_i/\tau_p \sim 10^{-5}$–$10^{-2}$ cm$^{-3}$ s$^{-1}$.

The concentration of droplets inside liquid and mixed clouds may change due to (a) secondary activation, (b) evaporation, (c) sedimentation, (d) collision–coalescence, and (e) droplet freezing. The secondary activation of droplets may occur if $u_z > u_z^+$, where $u_z^+$ is the threshold velocity required for activation of interstitial cloud condensation nuclei CCN (Korolev 1994). For typical $N_w\bar{r}_w$ the characteristic threshold velocity is $u_z^+ \sim 10^{-1}$–$10^0$ m s$^{-1}$. Numerical modeling showed that the rate of change of concentration during secondary activation may vary in the range $\Delta N_w/\Delta t \sim$ 5–20 cm$^{-3}$ s$^{-1}$ (Korolev 1994). These estimations suggest that the changes of droplet concentration due to secondary activation depending on the rate $\Delta N_w/\Delta t$ may result in a difference between $S_w$ and $S_{qsw}$.

The characteristic rate of the changes of the concentration due to collision–coalescence based on numerical modeling is of the order of $\Delta N_w/\Delta t \sim 10^{-4}$ to $-10^{-5}$ cm$^{-3}$ s$^{-1}$ (Pruppacher and Klett 1997), and therefore, does not play any significant role in the formation of the $S_{qsw}$. The sedimentation may both decrease the particle concentration due to their fallout of the cloud parcel and increase it due to new particles entering the same parcel. For spatially uniformly distributed cloud particles the balance of the decrease and increase of the droplet concentration due to sedimentation will be close to zero. Therefore, the effect of the sedimentation is expected to be negligible and it satisfies the condition (35). However, this may not be the case near the cloud edges, where the spatial inhomogeneity of droplets is high.

The entrainment of dry out-of-cloud air with subsequent mixing with the saturated in-cloud environment will result in a decrease of supersaturation followed by the droplets evaporation. The effect of the entrainment and mixing will be most significant near the cloud boundaries.

The freezing of liquid droplets will reduce the concentration of droplets and increase the concentration of ice particles. Unfortunately, at present, the rate of ice nucleation at different temperatures is poorly known. In situ measurements in wave clouds showed that the glaciation of a downstream part of the cloud occurs within tens of seconds (e.g., Cotton and Field 2002). That suggests that condition (35) is satisfied and the rate of natural nucleation of ice likely does not affect $S_{qsw}$ in liquid and mixed-phase clouds.

In ice clouds, the value $N_i/\tau_p$ is comparable to or may be much less than $\Delta N_i/\Delta t$ due to sedimentation, aggregation, and ice nucleation. Therefore, Eq. (20) should be used carefully for estimation of the supersaturation from $S_{qsi}$ in ice clouds.

Turbulent fluctuations may result in inhomogeneity of the droplet concentration (preferential concentration), which would cause perturbations of the supersaturation and nonuniform growth of cloud particles. Detailed studies by Vaillancourt et al. (2001, 2002) showed that, in cloud cores, the perturbation of supersaturation caused by preferential concentration is relatively small, and therefore, the effect of the preferential concentration can be neglected.

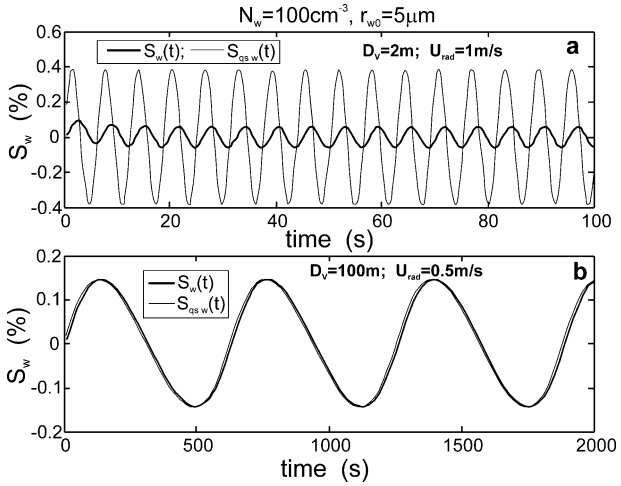


FIG. 17. Time variations of $S_{qsw}(t)$ and $S_w(t)$ in a vertically oscillating liquid cloud with (a) $\tau_p \ll \tau_t$, high-frequency vertical oscillations $D_v = 2$ m, $u_{vort} = 1$ m s$^{-1}$, $\tau_t = 1$ s; and (b) $\tau_p \gg \tau_t$, low-frequency oscillations $D_v = 100$ m, $u_{vort} = 0.5$ m s$^{-1}$, $\tau_t = 100$ s. For both clouds $N_w = 100$ cm$^{-3}$, $r_{w0} = 5$ $\mu$m; $\tau_p = 6.6$ s, $T(0) = 0$°C, $P(0) = 870$ mb. The vertical velocity was changed to $u_z = u_{vort} \sin(2tu_{vort}/D_v)$.

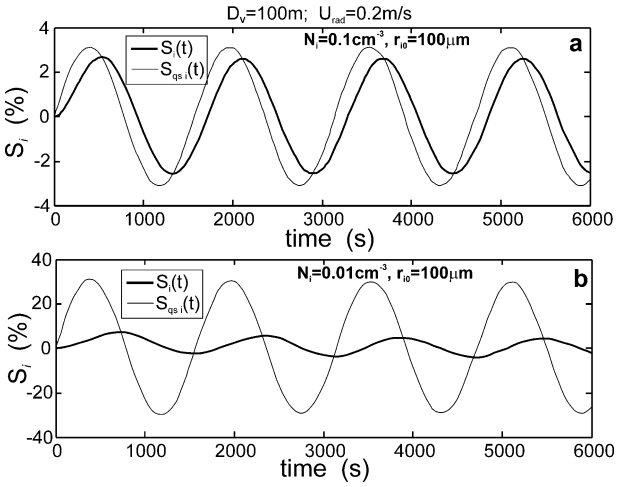


FIG. 18. Time variations of $S_{qsi}(t)$ and $S_i(t)$ in a vertically oscillating ice cloud with (a) $\tau_p \sim \tau_t$, $N_w = 0.1$ cm$^{-3}$, $r_{i0} = 10$ $\mu$m, $\tau_p = 171$ s; and (b) $\tau_p \gg \tau_t$, $N_i = 0.01$ cm$^{-3}$, $r_{i0} = 10$ $\mu$m; $\tau_p = 1710$ s. For both clouds, $D_v = 100$ m, $u_{vort} = 0.2$ m s$^{-1}$, $\tau_v = 250$ s, $T(0) = -35$°C; $P(0) = 360$ mb. The vertical velocity was changed to $u_z = u_{vort} \sin(2tu_{vort}/D_v)$.

### c. *Changes of vertical velocity and characteristic timescale*

The limitation for the vertical velocity for the quasi-steady supersaturation yields

$$\left|\frac{\Delta u_z}{\Delta t}\right| \ll \frac{u_z}{\tau_p}. \tag{36}$$

In real clouds, vertical velocity experiences continuous fluctuation due to turbulence, wave motions, or convection. Early works of Sedunov (1965), Mazin (1967), Kabanov and Mazin (1970), and Kabanov (1970), have studied the relation between the turbulent velocity fluctuations and supersaturation in the cloudy atmosphere. They showed the cloud droplets would accommodate the vapor, and the processes inside a cloud would be wet adiabatic if

$$\tau_p \ll \tau_t; \tag{37}$$

here $\tau_i \sim (L^2/\varepsilon)^{1/3}$ is the characteristic timescale of the vertical turbulent fluctuation. If $\tau_p \gg \tau_t$, then the response of the supersaturation on the vertical motion will be reduced. In this case the droplets, due to the condensational inertia, would not have enough time to adapt the water vapor and the processes inside such a parcel would follow the dry adiabat.

The characteristic timescale of turbulence $\tau_t$ may be considered as the time of a turnover of a turbulent vortex. In this case, $\Delta u_z$ can be estimated as $\Delta u_z \sim 2u_z$. Substituting this estimate into Eq. (36) results in Eq. (37).

The behavior of the supersaturation under the limits $\tau_p \ll \tau_t$ and $\tau_p \gg \tau_t$ can be illustrated by the following examples. Figure 17 shows temporal variations of $S_w(t)$ and $S_{qsw}(t)$ in a vertically oscillating parcel in a liquid cloud. The vertical velocity was changed as $u_z = u_{vort} \sin(\omega t)$, where $\omega = 2u_{vort}/D_v$; $D_v$ and $u_{vort}$ are the diameter and tangential velocity of the vortex, respectively. The characteristic time of such vertical fluctuations can be estimated as $\tau_t \sim 1/\omega$. Figure 17a demonstrates the case with $\tau_p > \tau_t$ ($\tau_t = 1$ s, $\tau_p = 6.6$ s). As a result the variations of the supersaturation $S_w$ are significantly less compared to $S_{qsw}(t)$. In this case $S_{qsw}(t)$ cannot be used to get an estimation of $S_w$. The frequency of the vertical fluctuations in Fig. 17a is too high and unlikely in natural clouds. However, such fluctuations might occur in the trails behind airplanes.

Figure 17b shows the case with $\tau_p \ll \tau_t$ ($\tau_t = 100$ s, $\tau_p = 6.6$ s). Such fluctuations ($D_v = 100$ m and $u_{vort} = 0.5$ m s$^{-1}$) are typical for stratocumulus, and its period ($2\pi D_v/u_{vort} \approx 10$ min) is close to that of the gravity waves. As seen, the $S_w(t)$ and $S_{qsw}(t)$ are nearly consistent, and $S_{qsw}(t)$ gives a very accurate estimate of $S_w(t)$.

Figure 18 shows time changes of $S_i(t)$ and $S_{qsi}(t)$ in the vertically oscillating parcel in a glaciated cloud with $\tau_p \sim \tau_t$($\tau_t = 250$ s, $\tau_p = 170$ s). The values of $N_i$, $\overline{r}_i$, $u_z$, and $D_v$ chosen in Fig. 18 could occur in cirrus clouds. The amplitudes of $S_i(t)$ and $S_{qsi}(t)$ for this cloud are about the same, though the phase of the oscillations is biased. It should be noted, that though $S_i(t)$ and $S_{qsi}(t)$ are different, frequency distribution of $S_{qsi}(t)$ calculated from a statistically significant ensemble of $N_i\overline{r}_i$ and $u_z$ would be about the same as the distribution of the actual $S_i$.

Figure 18b demonstrates the case when $\tau_p \gg \tau_t$($\tau_t =$

250 s, $\tau_p = 1710$ s). The $S(t)$ and $S_{qsi}(t)$ are significantly different as expected.

### d. Changes of particle sizes

The limitations on the changes of the cloud particle sizes may be defined from Eq. (15). Assuming that $S = S_{qsw}$, $t = \tau_p$, and substituting Eq. (16) and Eq. (18) into Eq. (15), yields

$$\frac{\overline{r}_w^4 N_w^2}{|u_z|} \gg \frac{2A_w a_0}{b_w^2}. \tag{38}$$

Equation 37 is valid for ice clouds, if the index "$w$" is replaced with "$i$." Differentiating $\overline{r}_w$ and $u_z$ in Eq. (38) by $t$, and using Eqs. (3) and (18) results in $|\Delta u_z/\Delta t| \ll 2u_z/\tau_p$, which is similar to Eq. (36), Thus, the limitation on the changes of the particle size reduces to the limitation on the vertical velocity.

### e. Characteristic spatial scale

The above consideration in sections 2–4 assumes that all processes are adiabatic. In real clouds, this assumption is violated due to entrainment and mixing. The entrainment and mixing would generate fluctuations of the supersaturation, which are not related to fluctuation of $u_z$, $N_w\overline{r}_w$, and $N_i\overline{r}_i$. After each event of entrainment and mixing, the supersaturation will recover to its quasi-steady value during a characteristic time $\tau_p$. If the characteristic spatial scale of the turbulent fluctuations $l_t \ll l_p$, then the quasi-steady approximation cannot be applied. Here,

$$l_p \sim \varepsilon^{1/2}\tau_p^{3/2} \tag{39}$$

is the characteristic *phase scale* (Mazin 1966; Kabanov and Mazin 1970); $\varepsilon$ is the turbulent energy dissipating rate. At the spatial scale $l_t \ll l_p$, the supersaturation $S_{qsw}(t)$ may be significantly different from the actual $S_w(t)$. Thus, we come to an important conclusion that the estimations of supersaturation from in situ measurements of $N_w\overline{r}_w$, $N_i\overline{r}_i$, and $u_z$, the averaging should be done over the scale $l > l_p$.

In stratocumulus the characteristic values $\varepsilon \sim 10^{-3}$ m$^2$ s$^{-3}$ (Mazin and Khrgian 1989) and $\tau_p \sim 10$ s result in $l_p \sim 1$ m. In convective clouds, $\varepsilon \sim 10^{-2}$–$10^{-1}$ m$^2$ s$^{-3}$ and $\tau_p \sim 10$ s result in $l_p \sim 3$–10 m.

## 9. Conclusions

In the framework of this study the following results were obtained.

1) An equation for quasi-steady supersaturation and the time of phase relaxation for the general case of mixed-phase clouds was obtained.
2) It is shown that the supersaturation $S(t)$ in a uniformly vertically moving cloud parcel asymptotically approaches, over time, the quasi-steady supersaturation $S_{qs}(t)$ calculated for current values of $u_z(t)$, $\overline{r}_w(t)$, $N_w(t)$, $\overline{r}_i(t)$, and $N_i(t)$. The characteristic time of the approach of $S(t)$ to $S_{qs}(t)$ is defined by the time of phase relaxation $\tau_p$ [Eqs. (13), (18), (21)]. This creates a theoretical basis for the use of $S_{qs}$ for estimating supersaturation in clouds from in situ measurements of $N_w\overline{r}_w$, $N_i\overline{r}_i$, and $u_z$ as was done by Warner (1968), Paluch and Knight (1984), and Politovich and Cooper (1988).
3) In estimating $S$ from in situ measurements, the averaging of $N_w\overline{r}_w$, $N_i\overline{r}_i$, and $u_z$ should be done over the scale $l > l_p$. The quasi-steady supersaturation $S_{qs}$ gives a good estimate of $S$ in liquid and mixed-phase clouds because usually $\tau_p < \tau_t$ in these clouds. In ice clouds, estimations of $S$ should be made with caution, because in many cases $\tau_p > \tau_t$.
4) Solution of the equation for the quasi-steady supersaturation suggests that for typical $N_w\overline{r}_w$ and $N_i\overline{r}_i$, the relative humidity in liquid and mixed phase clouds is close to the saturation over water, and the characteristic time of settling of the supersaturation ($\tau_p$) is of the order of seconds. In ice clouds the quasi-steady supersaturation is close to saturation over ice. However, for typical $N_i\overline{r}_i$ in ice clouds, the characteristic time of approaching of the supersaturation to its quasi-steady value may range from minutes to hours ($\tau_p > \tau_t$). Therefore, in situ measurements of the relative humidity in ice clouds may result in any value below the saturation over water; that is, it may be both higher or lower than saturation over ice.
5) Liquid water droplets can be activated in ice clouds with $N_i\overline{r}_i < 1$ cm$^{-3}$ at $u_z \sim 1$ m s$^{-1}$. The vertical turbulent and regular motions observed in natural clouds may maintain the cloud in mixed phase for a long time. The condition for the activation of liquid droplets and maintaining the cloud in mixed phase is determined by Eq. (22). This may be a possible explanation of the large observed fraction of mixed phase clouds.

In conclusion we would like to stress the importance that the integral radii should not be overlooked. The values of integral radii $N_w\overline{r}_w$ and $N_i\overline{r}_i$ define $S_{qsw}$ and $\tau_p$. Thus, the first moment of the cloud particle size distribution ($N\overline{r}$), similar to the second moment ($N\overline{r^2}$) defining optical properties of cloud, and the third moment ($N\overline{r^3}$) defining cloud water content, should be considered one of the main parameters in cloud physics.

*Acknowledgments.* We appreciate Prof. Roddy Rogers (National Science Foundation) for supporting this paper. Many thanks to Monika Bailey (Meteorological Service of Canada) for editing the text. The authors express gratitude to two anonymous reviewers for useful comments that help to improve the paper.

## APPENDIX A

### Supersaturation in a Vertically Moving Parcel

In the following consideration, the supersaturation is defined as

$$S_w = \frac{e - E_w}{E_w}, \tag{A1}$$

where $e$ is the water vapor pressure and $E_w$ is the saturated water vapor pressure. The rate of change of supersaturation in a vertically moving adiabatic parcel can be found by differentiating Eq. (A1):

$$\frac{dS_w}{dt} = \frac{1}{E_w}\frac{de}{dt} - \frac{e}{E_w^2}\frac{dE_w}{dt}. \tag{A2}$$

To find $de/dt$, we express the water vapor pressure as

$$e = q_v p \frac{R_v}{R_a}. \tag{A3}$$

Here, $p$ is the pressure of a dry air; $q_v = m_v/m_a$ is the mixing ratio of water vapor, that is, the mass of water vapor $m_v$ per mass of the dry air $m_a$. Differentiating Eq. (A3) gives

$$\frac{de}{dt} = \frac{R_v}{R_a} p \frac{dq_v}{dt} + \frac{R_v}{R_a} q_v \frac{dp}{dt}. \tag{A4}$$

Using the Clayperon–Clausius equation $dE_w/dT = L_w E_w/R_v T^2$, the changes of the saturated vapor pressure can be presented as

$$\frac{dE_w}{dt} = \frac{dE_w}{dT}\frac{dT}{dt} = \frac{L_w E_w}{R_v T^2}\frac{dT}{dt}. \tag{A5}$$

The term $dT/dt$ can be found from the energy conservation equation for an adiabatic parcel

$$c_p dT - R_a T \frac{dp}{p} - L_w dq_w - L_i dq_i = 0. \tag{A6}$$

Differentiating Eq. (A6) and substituting $dT/dt$ in Eq. (A5) yields

$$\frac{dE_w}{dt} = \frac{R_a L_w E_w}{p c_p R_v T}\frac{dp}{dt} + \frac{L_w^2 E_w}{c_p R_v T^2}\frac{dq_w}{dt} + \frac{L_i L_w E_w}{c_p R_v T^2}\frac{dq_i}{dt}. \tag{A7}$$

Substituting Eqs. (A4) and (A7) in Eq. (A1) results in

$$\frac{dS_w}{dt} = \frac{1}{E_w}\left(\frac{R_v}{R_a} p \frac{dq_v}{dt} + \frac{R_v}{R_a} q_v \frac{dp}{dt}\right) - \frac{e}{E_w^2}\left(\frac{R_a L_w E_w}{p c_p R_v T}\frac{dp}{dt} + \frac{L_w^2 E_w}{c_p R_v T^2}\frac{dq_w}{dt} + \frac{L_i L_w E_w}{c_p R_v T^2}\frac{dq_i}{dt}\right). \tag{A8}$$

Using the equation for quasi-hydrostatic approximation

$$\frac{dp}{dt} = -\frac{gp}{R_a T} u_z, \tag{A9}$$

the equation for the conservation of total water mass

$$\frac{dq_v}{dt} + \frac{dq_w}{dt} + \frac{dq_i}{dt} = 0, \tag{A10}$$

and Eqs. (A1) and (A3) to derive $dp/dt$, $dq_v/dt$, $e/E_w$, and $p$, respectively, and substituting in Eq. (A8) yields

$$\frac{1}{S_w + 1}\frac{dS_w}{dt} = \left(\frac{g L_w}{c_p R_v T^2} - \frac{g}{R_a T}\right) u_z - \left(\frac{1}{q_v} + \frac{L_w^2}{c_p R_v T^2}\right)\frac{dq_w}{dt} - \left(\frac{1}{q_v} + \frac{L_i L_w}{c_p R_v T^2}\right)\frac{dq_i}{dt}. \tag{A11}$$

In the above consideration, we used the following approximations: $p \cong p_m$, where $p$, $p_m$ are the pressures of dry and moist air, respectively. The quasi-hydrostatic approximation Eq. (A9) requires $u_z < 10$ m s$^{-1}$, which satisfies stratiform and shallow convective clouds conditions.

## APPENDIX B

### Numerical Model of Supersaturation in a Vertically Moving Cloud Parcel

The process of cloud-phase transformation in an adiabatic parcel can be described by a system of the following equations:

the pressure variation equation

$$\frac{dp}{dt} = -\frac{gpu_z}{R_a T}; \tag{B1}$$

the energy conservation equation

$$\frac{dT}{dt} = -\frac{gU_z}{c_p} + \frac{L_w}{(1 + q_v)c_p}\frac{dq_w}{dt} + \frac{L_i}{(1 + q_v)c_p}\frac{dq_i}{dt}; \tag{B2}$$

the water mass conservation equation

$$\frac{dq_v}{dt} + \frac{dq_w}{dt} + \frac{dq_i}{dt} = 0; \tag{B3}$$

the rate of change of the liquid droplets mass

$$\frac{dq_w}{dt} = 4\pi\rho_w A_w n_w r_w S_w; \tag{B4}$$

the rate of change of the ice particles mass

$$\frac{dq_i}{dt} = 4\pi c \rho_i A_i n_i r_i S_i; \tag{B5}$$

the rate of change of droplet size

$$\frac{dr_w}{dt} = \frac{A_w S_w}{r_w}; \quad \text{and} \tag{B6}$$

the rate of change of ice particle size

$$\frac{dr_i}{dt} = \frac{c A_i S_i}{r_i}. \tag{B7}$$

The explanation for the symbols is provided in ap-

pendix D. For $k(T)$, $L_w(T)$, and $L_i(T)$, the dependence on temperature was taken into account. For $D(T, P)$ both temperature and pressure were considered. The ice particles in the above model were assumed to be spheres, having initial size $r_i(t_0) = 1$ $\mu$m. Both droplets and ice particle were assumed to have monodisperse size distributions.

## APPENDIX C

### Equation for Supersaturation

In deriving Eq. (1) and Eq. (A11), the dependence of the term $1/q_v$ on the supersaturation was neglected. This approximation works very well for most cloudy situations in the troposphere. An accurate consideration of $q_v$ results in

$$q_v = \frac{eR_a}{pR_v} = (S_w + 1)\frac{E_w R_a}{pR_v}. \tag{C1}$$

Substituting Eq. (C1) into Eq. (1) yields

$$\frac{1}{S_w + 1}\frac{dS_w}{dt} = \left(\frac{gL_w}{c_p R_v T^2} - \frac{g}{R_a T}\right)u_z - \left(\frac{1}{S_w + 1}\frac{pR_v}{E_w R_a} + \frac{L_w^2}{c_p R_v T^2}\right)\frac{dq_w}{dt} - \left(\frac{1}{S_w + 1}\frac{pR_v}{E_w R_a} + \frac{L_i L_w}{c_p R_v T^2}\right)\frac{dq_i}{dt}. \tag{C2}$$

Substituting $dq_w/dt$ and $dq_i/dt$, similar to that in section 2, results in

$$\frac{1}{S_w + 1}\frac{dS_w}{dt} = \left(\frac{gL_w}{c_p R_v T^2} - \frac{g}{R_a T}\right)u_z - \left(\frac{1}{S_w + 1}\frac{pR_v}{E_w R_a} + \frac{L_i L_w}{c_p R_v T^2}\right)B_i^* N_i \bar{r}_i - \left[\left(\frac{1}{S_w + 1}\frac{pR_v}{E_w R_a} + \frac{L_w^2}{c_p R_v T^2}\right)B_w N_w \bar{r}_w + \left(\frac{1}{S_w + 1}\frac{pR_v}{E_w R_a} + \frac{L_i L_w}{c_p R_v T^2}\right)B_i N_i \bar{r}_i\right]S_w. \tag{C3}$$

Equation (C3) can be rewritten as

$$\frac{dS_w}{dt} = AS_w^2 - BS_w + C. \tag{C4}$$

Here, the following designations have been used:

$$A = -a_6 B_w N_w \bar{r}_w - a_5 B_i N_i \bar{r}_i; \tag{C5}$$

$$B = a_5 B_i^* N_i \bar{r}_i + (a_4 + a_6)B_w N_w \bar{r}_w + (a_4 + a_5)B_i N_i \bar{r}_i - a_0 u_z; \tag{C6}$$

$$C = a_0 u_z - (a_4 + a_5)B_i^* N_i \bar{r}_i; \tag{C7}$$

$$a_4 = \frac{pR_v}{E_w R_a}; \qquad a_5 = \frac{L_w L_i}{c_p R_v T^2}; \qquad a_6 = \frac{L_w^2}{c_p R_v T^2}.$$

In the frame-work of quasi-steady approximation ($\bar{r}_w$ = const and $\bar{r}_i$ = const), Eq. (C3) yields a solution

$$S_w = \frac{S_2 - S_1\dfrac{S_0 - S_2}{S_0 - S_1}\exp\left(-\dfrac{t}{\tau}\right)}{1 - \dfrac{S_0 - S_2}{S_0 - S_1}\exp\left(-\dfrac{t}{\tau}\right)}, \tag{C8}$$

where

$$S_{1,2} = \frac{B \pm \sqrt{B^2 - 4AC}}{2A} \quad \text{and} \tag{C9}$$

$$\tau = \frac{1}{A(S_2 - S_1)} = \frac{1}{\sqrt{B^2 - 4AC}}. \tag{C10}$$

As seen from Eq. (C8), when time $t$ increases the supersaturation, $S_w$ asymptotically approaches $S_2$, which will be referred to as quasi-steady supersaturation and denoted $S_{qsw}$:

$$S_{qsw} = \frac{B - \sqrt{B^2 - 4AC}}{2A}. \tag{C11}$$

For $N_w\bar{r}_w$, $N_i\bar{r}_i$, and $u_z$ typical for tropospheric clouds, $B \gg AC$. This allows an expansion of the expression under the square root sign in Eqs. (C10) and (C11). Then substituting Eqs. (C5)–(C7) yields

$$S_{qsw} \approx \frac{C}{B} = \frac{a_0 u_z - c_i^* N_i \bar{r}_i}{c_w N_w \bar{r}_w + c_i N_i \bar{r}_i - a_0 u_z} \quad \text{and} \tag{C12}$$

$$\tau_p \approx \frac{1}{B} = \frac{1}{c_w N_w \bar{r}_w + c_i N_i \bar{r}_i - a_0 u_z}. \tag{C13}$$

Here, $c_w = (a_4 + a_6)B_w$, $c_i = (a_4 + a_5)B_i + a_5 B_i^*$, and $c_i^* = (a_4 + a_5)B_i^*$. Comparisons show that Eq. (C12) and Eq. (C13) are close to Eqs. (12) and (13), respectively.

## APPENDIX D

### List of Symbols

| Symbol | Description | Units |
|---|---|---|
| $a_0$ | $\frac{g}{R_a T}\left(\frac{LR_a}{c_p R_v T} - 1\right)$ | $m^{-1}$ |
| $a_1$ | $\frac{1}{q_v} + \frac{L_w^2}{c_p R_v T^2}$ | — |
| $a_2$ | $\frac{1}{q_v} + \frac{L_w L_i}{c_p R_v T^2}$ | — |
| $a_3$ | $\frac{1}{q_v} + \frac{L_i^2}{c_p R_v T^2}$ | — |
| $a_4$ | $\frac{pR_v}{E_w R_a}$ | — |
| $a_5$ | $\frac{L_w L_i}{c_p R_v T^2}$ | — |
| $a_6$ | $\frac{L_w^2}{c_p R_v T^2}$ | — |
| $A_i$ | $\left[\frac{\rho_i L_i^2}{kR_v T^2} + \frac{\rho_i R_v T}{E_i(T) D}\right]^{-1}$ | $m^2\ s^{-1}$ |
| $A_w$ | $\left[\frac{\rho_w L_w^2}{kR_v T^2} + \frac{\rho_w R_v T}{E_w(T) D}\right]^{-1}$ | $m^2\ s^{-1}$ |
| $b_w$ | $a_1 B_w$ | $m^2\ s^{-1}$ |
| $b_i$ | $a_2 B_w$ | $m^2\ s^{-1}$ |
| $b_{i0}$ | $a_2 B_{w0}$ | $m^2\ s^{-1}$ |
| $b_i^*$ | $a_2 B_i^*$ | $m^2\ s^{-1}$ |
| $B_i$ | $\frac{4\pi\rho_i \xi c A_i}{\rho_a}$ | $m^2\ s^{-1}$ |
| $B_{i0}$ | $\frac{4\pi\rho_i c A_i}{\rho_a}$ | $m^2\ s^{-1}$ |
| $B_i^*$ | $\frac{4\pi}{\rho_a}\rho_i(\xi - 1) c A_i$ | $m^2\ s^{-1}$ |
| $B_w$ | $\frac{4\pi\rho_w A_w}{\rho_a}$ | $m^2\ s^{-1}$ |
| $c$ | Ice particle shape factor characterizing capacitance $0 < c \leq 1$ ($c = 1$ for spheres) | — |
| $c_p$ | Specific heat capacity of moist air at constant pressure | $J\ kg^{-1}\ K^{-1}$ |
| $c_i$ | $(a_4 + a_5)B_i + a_5 B_i^*$ | $m^2\ s^{-1}$ |
| $c_i^*$ | $(a_4 + a_5)B_i^*$ | $m^2\ s^{-1}$ |
| $c_w$ | $(a_4 + a_6)B_w$ | $m^2\ s^{-1}$ |
| $D$ | Coefficient of water vapor diffusion in the air | $m^2\ s^{-1}$ |
| $e$ | Water vapor pressure | $N\ m^{-2}$ |
| $E_i$ | Saturation vapor pressure above flat surface of ice | $N\ m^{-2}$ |
| $E_w$ | Saturation vapor pressure above flat surface of water | $N\ m^{-2}$ |
| $f_w(r_w)$ | Size distribution of cloud droplets normalized on unity | $m^{-1}$ |
| $f_i(r_i)$ | Size distribution of ice particles normalized on unity | $m^{-1}$ |
| $g$ | Acceleration of gravity | $m\ s^{-2}$ |
| $k$ | Coefficient of air heat conductivity | $J\ m^{-1}\ s^{-1}\ K^{-1}$ |
| $L_i$ | Latent heat for ice sublimation | $J\ kg^{-1}$ |
| $L_w$ | Latent heat for liquid water evaporation | $J\ kg^{-1}$ |
| $l_p$ | Characteristic spatial phase scale | m |
| $m_i$ | Mass of a single ice particle | kg |
| $N_i$ | Concentration of ice particles | $m^{-3}$ |
| $N_w$ | Concentration of liquid droplets | $m^{-3}$ |
| $n_i$ | $N_i/\rho_a$ number of ice particles per unit mass or dry air | $kg^{-1}$ |
| $n_w$ | $N_w/\rho_a$ number of liquid droplets per unit mass or dry air | $kg^{-1}$ |
| $p$ | Pressure of moist air | $N\ m^{-2}$ |
| $p_a$ | Pressure of dry air | $N\ m^{-2}$ |
| $r_i$ | Half of a maximum linear dimension of an ice particle | m |
| $r_w$ | Liquid droplet radius | m |
| $R_a$ | Specific gas constant of moist air | $J\ kg^{-1}\ K^{-1}$ |
| $R_v$ | Specific gas constant of water vapor | $J\ kg^{-1}\ K^{-1}$ |
| $q_i$ | Ice water mixing ratio (mass of ice per 1 kg of dry air) | — |
| $q_v$ | Water vapor mixing ratio (mass of water vapor per 1 kg of dry air) | — |
| $q_w$ | Liquid water mixing ratio (mass of liquid water per 1 kg of dry air) | — |
| $S_i$ | $e/E_i - 1$, supersaturation over ice | — |
| $S_w$ | $e/E_w - 1$, supersaturation over water | — |
| $S_{qsi}$ | Quasi-steady supersaturation with respect to ice | — |
| $S_{qsw}$ | Quasi-steady supersaturation with respect to water | — |
| $S_i^*(t)$ | Solution of Eq. (9) for supersaturation over ice when $\bar{r}_i$ = constant and $\bar{r}_w$ = constant | — |
| $S_w^*(t)$ | Solution of Eq. (9) for supersaturation over water when $\bar{r}_i$ = constant and $\bar{r}_w$ = constant | — |
| $T$ | Temperature | K |
| $t$ | Time | s |
| $u_z$ | Vertical velocity | $m\ s^{-1}$ |
| $W_i$ | Ice water content | $kg\ m^{-3}$ |
| $W_w$ | Liquid water content | $kg\ m^{-3}$ |
| $\gamma_a$ | Dry adiabatic lapse rate | $K\ m^{-1}$ |
| $\varepsilon$ | Turbulent energy dissipating rate | $m^2\ s^3$ |
| $\rho_a$ | Density of the dry air | $kg\ m^{-3}$ |
| $\rho_i$ | Density of an ice particle | $kg\ m^{-3}$ |
| $\rho_w$ | Density of liquid water | $kg\ m^{-3}$ |
| $\tau_p$ | Time of phase relaxation | s |
| $\tau_t$ | Characteristic timescale of the vertical turbulent velocity fluctuations | s |
| $\tau_{gl}$ | Glaciating time of a mixed-phase cloud | s |
| $\xi$ | $E_w/E_i$ | — |

## REFERENCES


Bergeron, T., 1935: On the physics of clouds and precipitation. *Proc. V^e Assemblée Générale de l'Union Géodésique et Geophysique Internationale*, Lisbon, Portugal, International Union of Geodesy and Geophysics. 156–180.

Cotton, R. J., and P. R. Field, 2002: Ice nucleation characteristics of an isolated wave cloud. *Quart. J. Roy. Meteor. Soc.*, **128,** 2417–2439.

Findeisen, W., 1938: Kolloid-meteorologische Vorgänge bei Neiderschlags-bildung. *Meteor. Z.*, **55,** 121–133.

Heymsfield, A. I., 1975: Cirrus uncinus generating cells and the evolution of cirrdorm clouds. Part III: Numerical computations of the growth of the ice phase. *J. Atmos. Sci.*, **32,** 820–830.

Howell, W. E., 1949: The growth of cloud drops in uniformly cooled air. *J. Meteor.*, **6,** 139–149.
Juisto, J. E., 1971: Crystal development and glaciation of a supercooled cloud. *J. Rech. Atmos.,* **5,** 69–86.
Kabanov, A. S., 1970: On the spectrum of the turbulence in the free atmosphere with the phase transition of water (in Russian). *Tr. TsAO,* **97,** 103–118.
——, and I. P. Mazin, 1970: The effect of turbulence on phase transition in clouds (in Russian). *Tr. TsAO,* **98,** 113–121.
——, ——, and V. I. Smirnov, 1971: Water vapor supersaturation in clouds (in Russian). *Tr. TsAO,* **95,** 50–61.
Korolev, A. V., 1994: A study of bimodal droplet size distributions in stratiform clouds. *Atmos. Res.* **32,** 143–170.
——, and G. A. Isaac, 2003: Phase transformation in mixed phase clouds. *Quart. J. Roy. Meteor. Soc.,* **129,** 19–38.
——, ——, S. G. Cober, J. W. Strapp, and J. Hallett, 2003: Observation of the microstructure of mixed phase clouds. *Quart. J. Roy. Meteor. Soc.,* **129,** 39–66.
Mazin, I. P., 1966: On temperature and humidity stratification in clouds (in Russian). *Tr. TsAO,* **71,** 3–15.
——, 1967: Interrelation between fluctuations of supersaturation in clouds and fluctuations of temperature and vertical velocity (in Russian). *Tr. TsAO,* **79,** 3–8.
——, 1968: Effect of phase transition on formation of temperature and humidity stratification in clouds. *Proc. Int. Conf. on Cloud Physics.* Toronto, Ontario, Canada, Amer. Meteor. Soc., 132–137.
——, 1983: Phase changes in clouds. *Soviet Meteorology and Hydrology,* No. 7, Allerton Press, 26–34.
——, and A. Kh. Khrgian, Eds., 1989: *Handbook of Clouds and Cloudy Atmosphere.* Gidrometeoizdat, 647 pp.
——, V. I. Silaeva, and M. A. Strunin, 1984: Turbulent fluctuations of the horizontal and vertical air velocity components in different types of clouds. *Izv. Akad. Nauk SSSR, Fiz. Atmos. Okeana,* **20,** 6–11.
Mordy, W., 1959: Computations of the growth by condensation of a population of cloud droplets. *Tellus,* **11,** 16–44.
Paluch, I. R., and Ch. A. Knight, 1984: Mixing and evolution of cloud droplet size spectra in vigorous continental cumulus. *J. Atmos. Sci.,* **41,** 1801–1815.
Politovich, M. K., and W. A. Cooper, 1988: Variability of the supersaturation in cumulus clouds. *J. Atmos. Sci.,* **45,** 1651–1664.
Pruppacher, H. R., and J. D. Klett, 1997: *Microphysics of Clouds and Precipitation.* Kluwer Academic, 976 pp.
Rogers, R. R., 1975: An elementary parcel model with explicit condensation and supersaturation. *Atmosphere,* **13,** 192–204.
Sedunov, Yu. S., 1965: Fine cloud structure and its role in the formation of the cloud spectrum. *Atmos. Oceanic Phys.,* **1,** 416–421.
——, 1974: *Physics of Drop Formation in the Atmosphere.* John Wiley & Sons, 234 pp.
Squires, P., 1952: The growth of cloud drops by condensation. *Aust. J. Sci. Res.,* **5,** 66–86.
Vaillancourt, P. A., M. K. Yau, and W. W. Grabowski, 2001: Microscopic approach to cloud droplet growth by condensation. Part I: Model description and results without turbulence. *J. Atmos. Sci.,* **58,** 1945–1964.
——, ——, P. Bartello, and W. W. Grabowski, 2002: Microscopic approach to cloud droplet growth by condensation. Part II: Turbulence, clustering, and condensational growth. *J. Atmos. Sci.,* **59,** 3421–3435.
Warner, J., 1968: The supersaturation in natural clouds. *J. Rech. Atmos.,* **3,** 233–237.
Wegener, A., 1911: *Thermodynamik der Atmosphäre* (in German). J. A. Barth, 331 pp.